coatings

MDPI

Review

Passive Layers and Corrosion Resistance of Biomedical Ti-6Al-4V and β-Ti Alloys

Patrizia Bocchetta [1,*], Liang-Yu Chen [2], Juliana Dias Corpa Tardelli [3], Andréa Cândido dos Reis [3], Facundo Almeraya-Calderón [4] and Paola Leo [1,*]

1 Department of Innovation Engineering, University of Salento, Via per Monteroni, 73100 Lecce, Italy
2 School of Materials Science and Engineering, Jiangsu University of Science and Technology, Mengxi Road 2#, Zhenjiang 212003, China; lychen@just.edu.cn
3 Department of Dental Materials and Prosthesis, School of Dentistry of RibeirãoPreto, University of São Paulo (USP), Ribeirão Preto 14040-904, Brazil; juliana.tardelli@usp.br (J.D.C.T.); andreare@forp.usp.br (A.C.d.R.)
4 FIME-Centro de Investigación e Innovación en Ingeniería Aeronáutica (CIIIA), Universidad Autonoma de Nuevo Leon, Av. Universidad s/n, Ciudad Universitaria, San Nicolás de los Garza 66455, Mexico; facundo.almerayacld@uanl.edu.mx
* Correspondence: patrizia.bocchetta@unisalento.it (P.B.); paola.leo@unisalento.it (P.L.)

Abstract: The high specific strength, good corrosion resistance, and great biocompatibility make titanium and its alloys the ideal materials for biomedical metallic implants. Ti-6Al-4V alloy is the most employed in practical biomedical applications because of the excellent combination of strength, fracture toughness, and corrosion resistance. However, recent studies have demonstrated some limits in biocompatibility due to the presence of toxic Al and V. Consequently, scientific literature has reported novel biomedical β-Ti alloys containing biocompatible β-stabilizers (such as Mo, Ta, and Zr) studying the possibility to obtain similar performances to the Ti-6Al-4V alloys. The aim of this review is to highlight the corrosion resistance of the passive layers on biomedical Ti-6Al-4V and β-type Ti alloys in the human body environment by reviewing relevant literature research contributions. The discussion is focused on all those factors that influence the performance of the passive layer at the surface of the alloy subjected to electrochemical corrosion, among which the alloy composition, the method selected to grow the oxide coating, and the physicochemical conditions of the body fluid are the most significant.

Keywords: biomedical titanium alloys; Ti-6Al-4V alloys; β-Ti alloys; passive layer; corrosion in human body; biocorrosion

check for updates

Citation: Bocchetta, P.; Chen, L.-Y.; Tardelli, J.D.C.; Reis, A.C.d.; Almeraya-Calderón, F.; Leo, P. Passive Layers and Corrosion Resistance of Biomedical Ti-6Al-4V and β-Ti Alloys. *Coatings* **2021**, *11*, 487. https://doi.org/10.3390/coatings11050487

Academic Editor: Grzegorz Dercz

Received: 24 March 2021
Accepted: 16 April 2021
Published: 21 April 2021

Publisher's Note: MDPI stays neutral with regard to jurisdictional claims in published maps and institutional affiliations.

Copyright: © 2021 by the authors. Licensee MDPI, Basel, Switzerland. This article is an open access article distributed under the terms and conditions of the Creative Commons Attribution (CC BY) license (https://creativecommons.org/licenses/by/4.0/).

1. Introduction

Titanium (Ti) and its alloys represent the material of choice for biomedical implants; however, the human body is a challenging environment for any biomaterials due to metabolic, immunological, biochemical, and microbiological processes, which interfere with its resistance to corrosion [1–4]. Furthermore, the corrosion resistance of Ti alloys depends on their composition, microstructure, and surface treatment [1,5–8]. Therefore, particles and ions released by the corrosive phenomenon can accumulate in the peri-implant bone and result in decreased functionality, mechanical integrity, and loss of implant mass with consequences on its useful life by increasing the probability of failure, bone resorption, infections, and loosening, or cause systemic migration to various organs, which can cause long-term health problems [1,2,4,6,9,10].

Titanium has electrochemical properties superior to other metals due to the passive surface TiO_2 layer; nevertheless, the oral cavity is a dynamic environment influenced by the variation of charge, pH, and corrosive products of dietary metabolism and biofilm, which can provide accelerated corrosion with consequent damage to the survival of the

implant by interfering in the thickness of the oxide layer and the process of repassivation [1,2,4,6,11–13]. According to Mischler et al. [14], the corrosion potential is influenced by the formation of the passive oxide layer, corrosion rate, temperature, and electrolyte. Therefore, the biocompatibility of Ti alloys is strictly correlated to the interaction between the physicochemical, morphological, and mechanical properties of the Ti oxide film grown spontaneously on the implant surface, accountable for its corrosion resistance, and the biological environment [1,4,6,9]. Recent studies have demonstrated the genotoxic and cytotoxic potential of nano TiO_2 particles; this has motivated researchers to study the influence of the chemical composition of Ti alloys on bone–implant interaction for the best recommendation of these in all procedures in which it is required [6,9,10,15–17].

The Ti-6Al-4V alloy (one of α + β type of Ti alloys) is the most used because it has excellent mechanical properties. Still, it is subject to discussion, because its elements of Al and V are associated with local inflammation, allergic reactions, carcinogenic effects, and neurological disorders [2,4–6,9,10,18–20]. Meanwhile, because its elastic modulus (110GPa) is greater than that of the bone (<30 GPa), it leads to peri-implant bone loss; yet under physiological conditions, it is hard to maintain the integrity of the protective oxide coating that corrodes by losing thickness and adherence [9,18]. Thus, in the last three decades, the development of β-Ti alloys with elements considered noncytotoxic—Nb, Ta, Zr, and Mo—has grown considerably because they promote excellent biocompatibility, low Young's modulus, low cost, and resistance to corrosion [4,5,9,10,18]. It should be noted that in studies, which evaluated the alloys under physiological conditions, the oxides Nb_2O_5, Ta_2O_5, and ZrO_2 showed better stability and corrosion resistance than TiO_2 containing Al and V [5,9,21–23].

Titanium alloys can be obtained by casting, electron beam fusion or plasma arc fusion, galvanization, and additive manufacturing, the latter having received great attention in recent years for allowing freedom during the construction of the structure at a fast speed [4,9–11,24]. However, many questions are raised concerning the clinical applicability of manufactured parts because they have a different microstructure from castings, which interferes with their mechanical properties; therefore, this difference, coupled with constant cyclic stresses to which the implants are subjected, can provide unexpected performance in the simulated body fluids according to Sharma et al. [11]. Furthermore, different surface treatments are the target of research to improve the biocompatibility of alloys and their electrochemical properties such as heat treatment, magnetron sputtering, plasma electrolytic oxidation, and galvanostatic anodization, which show promising results for improving the protection of the layered oxide when producing thicker, more stable, and resistant films on the surface of alloys [1,2,4,18,20,25].

The microstructure of the Ti alloys can be modified by heat treatment, thermomechanical processing, and electroshocking treatment, which improve the mechanical properties through microstructural refinement that change the grain structure and size to ultrafine and even to nanodimensions [26–28]. Thus, considering the advantages of altering the microstructure, the need for researchers to develop a simple and efficient microstructural transformation method to improve the properties of Ti alloys is emphasized [26].

Among the available methods to deposit or grow protective coatings on Ti alloys before implantation, this review focus on those producing an oxide layer by metal oxidation, such as electrochemical anodization (EA) and plasma electrolytic oxidation (PEO). EA is a low-cost and rapid method to grow passive layers on the Ti alloy surface and allow the precise tuning of thickness, composition, morphology, and general properties of the coating by simply controlling the applied potential or current density and the electrolyte composition. EA has recently attracted interest in the biomedical field because of the possibility to grow highly ordered and controlled titania nanotubes coatings that show high corrosion resistance and great adhesion and functionality of the osteoblast cell; they also favor hydroxyapatite formation and tissue integration and allow high protein adsorption [22,29]. At high applied voltages under micro-arc phenomena, electrochemical anodization is called plasma electrolytic oxidation (PEO). This method produces a titanium oxide porous

structure strongly adherent to the alloy exposing Ti-OH functional groups and oxygen vacancies to the external solution showing corrosion resistance, biological, and antibacterial activity at the same time. Moreover, calcium and phosphorus ions can be incorporated into the oxide coating if relevant electrolyte conditions are selected [22,25].

Patents and scientific articles are published continuously, presenting the β-Ti alloys as promising when compared to the most widely used Ti-6Al-4V alloy, which is the subject of discussion due to its electrochemical products [5,6,9]. Therefore, this review aims to discuss substantial literature results on metallurgical, compositional, and electrochemical aspects of Ti-6Al-4V and β-type Ti alloys in biomedical environments, clarifying the key role of the passive layer (pre-formed or formed in situ) and its electrochemical dynamics in the human body environment.

2. Biomedical Titanium Alloys

Ti alloys exhibit high specific strength (i.e., the ratio between yield strength and density) and outstanding corrosion resistance due to the presence of a stable and protective oxide layer, (mainly consisted of TiO_2). In the human body environment, a passive film is spontaneously formed and rapidly rebuilt in case of breakings, hence the alloy is protected against further corrosion process [5–31].

Pure titanium possesses a hexagonal close-packed (hcp) structure at room temperature, named α phase. The phase transformation from α hcp structure to β body-centered cubic (bcc) structure occurs at the β transus temperature (883 °C). In the case of alloys, the β transus temperature depends on the chemical nature and composition of the alloying elements, which are commonly classified into α-stabilizers (such as Al, C, and O) and β-stabilizers (such as V, Mo, Ta, and Nb). The β transus temperature is reduced as the amount of β-stabilizer increases (Figure 1a). Ti alloys are generally classified on the base of their structure, namely α, (α + β), and β-type, that change depending on β-stabilizer concentration. Accordingly, different regions of existence can be identified in the β isomorphous phase diagram (Figure 1b) [5,32–34].

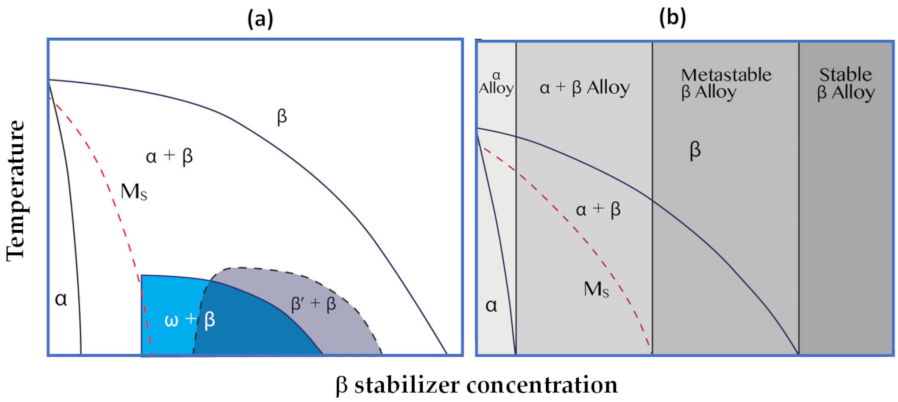

Figure 1. (**a**) Classification of Ti alloy as a function of β stabilizer concentration. (**b**) Scheme of metastable (ω + β) and (β′ + β) phase field [32].

α-type Ti alloys, consist of CP–Ti (commercially pure) and alpha alloys that, upon annealing well below the β transus, contain only a small volume fraction of beta phase (2–5 vol%) (Figure 1a). The alpha phase alloys are strengthened by solid solutioning (both by interstitial and substitutional element), refinement strengthening, and precipitation hardening. The strength of CP-Ti increases with increasing the amount of oxygen from 0.18% in grade 1 to 0.4% in grade 4 (Table 1), while the elastic moduli remain fixed and equal to 105 GPa. CP–Ti is the first generation of biomedical materials for dental and medical applications, but its mechanical properties (Table 1) restrain its use to that conditions that require high mechanical resistance. For this reason, titanium alloys have been studied as possible substitutes for CP titanium [5,32–34].

Table 1. Mechanical properties of Ti and Ti alloys for orthopedic implants. Reprinted from [5], copyright (2019), with permission from John Wiley and Sons.

Materials	$\sigma_{0.2}$ [MPa]	σ_{UTS} [MPa]	E [GPa]	ε_{max} [%].
α-type	-	-	-	-
CP-Ti grade 1	170	240	105	24
CP-Ti grade 2	275	345	105	2.20
CP-Ti grade 3	380	445	105	18
CP-Ti grade 4	480	550	105	15
(α + β)-type	-	-	-	-
T-6Al-4V (annealed)	825–869	895–930	110–114	6–10
T-6Al-4V ELI (mil annealed)	795–875	960–965	101–110	10–15
T-6Al-4V	795	860	105	10
T-6Al-4V	820	900	110	6
T-6Al-4V	585	690	100	15
β-type	-	-	-	-
Ti-13Nb-13Zr (aged)	836–908	973–1037	79–84	42–44
Ti-12Mo-6Zr-2Fe (annealed)	1000–1060	1060–1100	74–85	18–22
Ti-15Mo (annealed)	544	874	78	21
Ti-15Mo-5Zr-3Al (annealed)	838	852	80	25
Ti-15Mo-5Zr-3Al (ST)	1000–1060	1060–1100	-	18–22
Ti-15Mo-2.8Nb-0.2Si-0.260 (annealed)	945–987	979–999	83	16–18
Ti-16Nb-10Hf	736	851	81	10
Ti-35.5Nb-7.3-Zr-5.7-Ta	793	827	55–66	20
Ti-29Nb-13Ta-4.6Zr (aged)	864	911	80	13.2
Ti-24Nb-4Zr-8Sn (Hot rolled)	700	830	46	15.0
Ti-24Nb-4Zr-8Sn (hot forged)	570	755	55	13.0
Ti-9Mn	1023	1048	94	19.0
Ti-6Mn-4Mo	1090	1105	89	15.0
Ti-10Fe-10Ta-4Zr	960	1092	-	6.0
Ti-12Cr	-	760	65	18.5
Ti-36Mb-2Ta-3Zr-0.3O	670–1150	835–1180	32	6.5–12.9
Ti-24Nb-0.5O	665	810	54	22
Ti-24Nb-0.5N	665	665	43	13
Ti23Nb-0.7Ta-2Zr	280	400	55	33
Ti-23Nb-0.7Ta-2Zr-1.2O	830	880	60	14

$\sigma_{0.2}$, σ_{UTS}, and E, ε_{max} are yield strength, ultimate tensile strength, elastic modulus, and ultimate strain. ST = solution treated.

(α + β) Ti alloys have a higher content of β-stabilizers (Figure 1a), possess about 5–30 vol% of β, and transform martensitically upon fast cooling from beta field to room temperature. Hence, different microstructures can be obtained according to different thermal or thermomechanical cycles in order to optimize the mechanical properties of these alloys [5,32–34]. Figure 2 are shown four different microstructures for the (α + β)-type Ti-6Al-4V alloy, which is the most widely used biomedical alloy [5,33,35]. The lamellar microstructure (Figure 2a) supplies higher values of fracture toughness [32,33] compared to the martensitic (Figure 2b), bimodal (Figure 2c), and equiaxed microstructure (Figure 2d). The different microstructure/mechanical properties of Ti-6Al-4V affect the corrosion behavior of the alloy.

Specifically, the high hardness value (410 HV) of a martensitic Ti-6Al-4V improves its corrosion resistance with respect to the soft (α + β)-type microstructure (394 HV) because it permits a higher adherence of the oxide layer to the alloy [36]. Moreover, the occurrence of two-phase microstructure, such as the lamellar microstructure (Figure 2a), reduces the corrosion behavior due to the solute partitioning between α and β lamellae and the resultant galvanic interaction between the two phases [37].

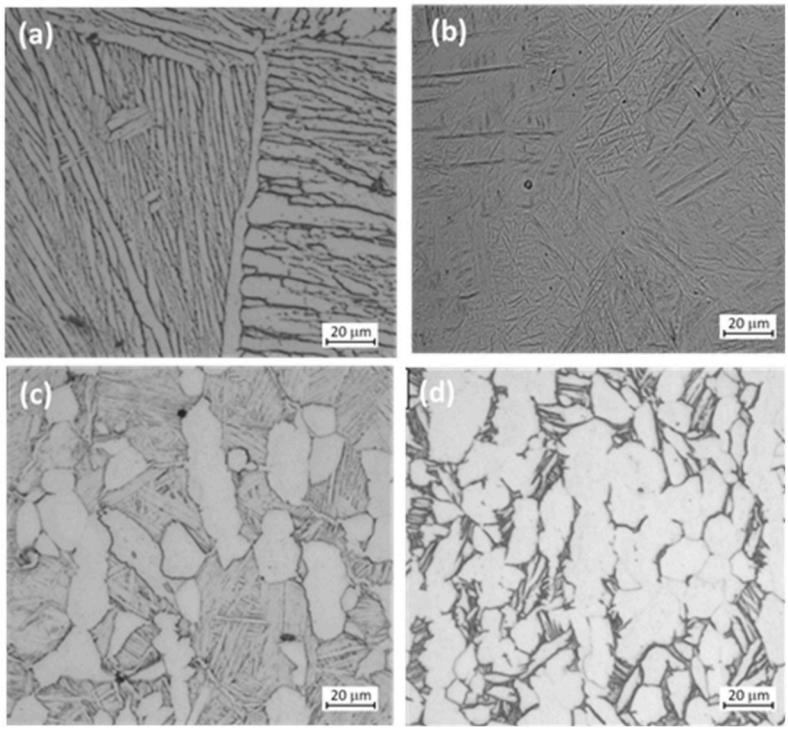

Figure 2. Microstructure of Ti-6Al-4V alloy. (**a**) Lamellar, (**b**) martensitic, (**c**) bimodal microstructure with alpha grains (white) and transformed microstructure into prior β grain, and (**d**) equiaxed alpha grains (white) and intergranular beta at the alpha grain boundary. Panels (**a**,**c**,**d**) reproduced under the Creative Commons Attribution License from [33].

Therefore, both the higher hardness and the absence of solute partition for the martensitic microstructure of Ti-6Al-4V (Figure 2b) improve its corrosion resistance [36,37].

Passivation of Ti alloy generates oxide coatings mainly composed of TiO_2 and, depending on the environmental conditions, morphologically constituted by a two-layer structure: the inner layer is compact, whereas the outer one is porous [25–31,35,36]. The corrosion resistance is mainly due to the inner layer that hinders the metal dissolution and increases with its thickness [5,31,36,38], while the outer porous layer favors osteointegration [28,34]. In the porous layer of the passive film, low contents of aluminum and vanadium oxides (Al_2O_3 and V_2O_5) are also present [38–40]. Both the Al and V oxides dissolve and deteriorate the passivity of Ti-6Al-4V [36,41,42]. The released Al and V ions are toxic and can lead to Alzheimer's disease and peripheral neuropathy [43,44]. Vanadium is toxic also in the oxide state [28,34,43,44].

In order to overcome the harmfulness of V, biomedical Ti alloys without V have been developed. For example, the biomedical (α + β)-type Ti–6Al–7Nb (Table 1). Electrochemical tests show that both Ti-6Al-4V and Ti–6Al–7Nb exhibit the same behavior in terms of corrosion resistance [39].

Although the high elastic modulus in CP-Ti and (α+β)-type Ti alloys is useful in terms of corrosion resistance [36], its value (Table 1) is very different with respect to that of human body bones, as shown in Table 2.

This difference can cause bone resorption and implant loosening due to the stress-shield effect (the elastic behavior mismatch between the implant and the adjacent bone) [5,34]. The goal of eliminating toxicity, improving the corrosion resistance of biomedical Ti alloys, and reducing the stress-shield effect has led to the development of β-type Ti alloys with nontoxic β stabilizers (such as Nb, Mo, Ta, and Zr) and elastic modulus closer to those of the human bones (Table 2) [5,34].

Table 2. Tensile properties of human cortical bones. Reprinted from [5], copyright (2019), with permission from John Wiley and Sons.

Bone	Age	N	n	σ_{UTS} [MPa]	E [GPa]	ε_{max} [%]	ρ [g cm^3]
Fibula	41.5	17	20	100	19.2	2.10	1.91
Fibula	71	17	16	80	15.2	1.19	1.73
Humerus *	15–89	64	27	149	15.6	2.20	1.77
Humerus **	15–89	64	16	151	16.1	1.90	1.72
Tibia	41.5	17	67	106	18.9	1.76	1.96
Tibia	71	17	34	84	16.2	1.56	1.83
Tibia	20–89	28	123	156	23.8	3.09	–
Femur	41.5	17	35	102	14.9	1.32	1.91
Femur	71	17	35	68	13.6	1.07	1.85
Femur *	15–89	64	29	141	15.2	2.00	1.90
Femur *	15–89	64	30	134	15.0	1.80	1.80
Femur	20–89	33	178	132	16.8	2.83	–

N is the number of tested bones and n is the number of samples obtained from the tested bones, σ_{UTS} is ultimate tensile strength, E is elastic modulus, ε_{max} is ultimate tensile strain, ρ is density, * refers to male and ** to female.

Titanium β alloys studied for biomedical applications fall in the (α + β) phase region of the phase diagram of Figure 1a. They are named metastable β alloys because of the ability to maintain the β phase at room temperature after fast cooling from the β phase region.

The amount of metastable-retained β phase increases with the number of beta stabilizer elements. That metastable beta phase can be aged at a low temperature after quenching and decomposition in different precipitates according to the amount of stabilizer (Figure 1b). For medium alloying content, those precipitates are named as ω, while for concentrated alloy are named as β′. The separation of ω and β′ leads to low ductility and fracture toughness. Hence, beta Ti alloys are aged at a higher temperature to precipitate incoherent particles of the stable α phase to increase both yield and fracture toughness [5,32–34].

For example, the yield stress of the β type biomedical Ti-29Nb-13Ta-4.6Zr alloy (also called TNTZ) in the solution-treated condition (metastable β phase) is equal to 600 MPa and is increased by aging 72 h at 300, 325, and 400 °C, as shown in Figure 3 [32,45]. In Table 1, the mechanical properties of the biomedical Ti-15Mo-5Zr-3Al in the aged state with respect to the solution are shown, indicating a significant increase of both yield and ultimate tensile stress due to the aged microstructure. A double temperature aging treatment can be also applied to obtain a more homogeneous distribution of incoherent particles of the stable α phase using ω or β′ particles as precursor and nucleation sites [32,33]. For example, pre-aging the TNTZ alloy at 260 °C for 4 h before the aging treatment at 427 °C for 8 h leads to much higher yield stress with respect to the one-step aging treatment at 427 °C for 8h [32,46,47].

Additive manufacturing (AM) technologies are widely used in the biomedical industry because they offer the opportunity of customization of the prostheses by adding thin layers of materials guided by a digital model. In particular, AM powder bed fusion techniques, such as selective laser melting and electron beam melting, use high-density energy beam to selectively melt a layer of powder by fast heating/cooling rate [5]. This method induces very fine microstructure, leading to comparable, or even better, mechanical properties of Ti alloys with respect to the counterparts obtained by conventional processes (a quantitative comparison can be found in Tables 6 and 7 in Ref. [5]).

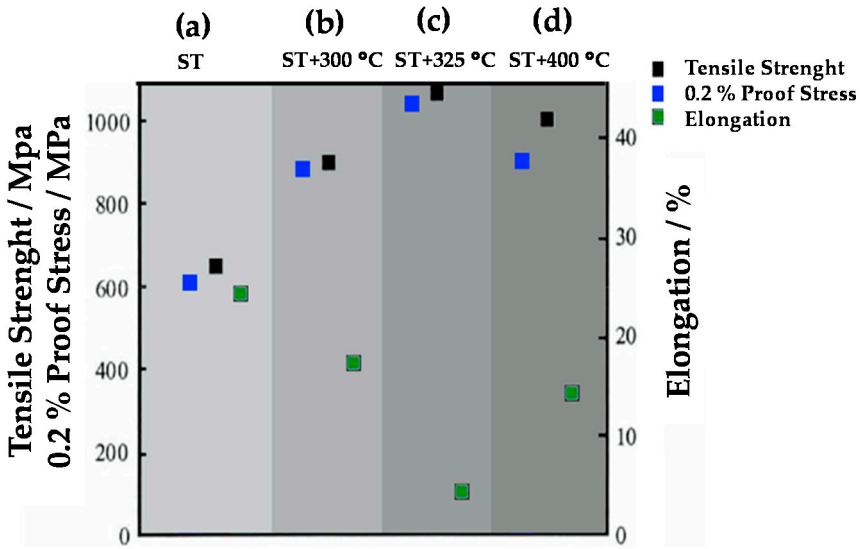

Figure 3. Tensile properties of TNTZ (Ti-29Nb-13Ta-4.6Zr) in a solution state (**a**) and after aging for 72 h at 300 °C (**b**), 325 °C (**c**), and 400 °C (**d**) [32,45].

In most β metastable Ti alloys, the elements such as Nb, Ta, and Zr lead to the formation of oxides (Nb_2O_5, ZrO_2, and Ta_2O_5) in the passive film, which have higher stability than the Al and V oxides and therefore increase the corrosion resistance of the alloy [47,48]. Regardless, the role of the microstructure on corrosion resistance is also significant [8,22,36,38]. For example, Ti–35Nb–7Zr–5Ta (TiOsteum) in metastable β state has shown an excellent corrosion behavior with respect to Ti-6Al-4V mill annealed state due to the presence of Nb_2O_5, ZrO_2, and Ta_2O_5 in the passive film and to the homogenous single-phase microstructure [8]. In another study [22], Ti–6Al–4V with equiaxed microstructure, exhibits a better corrosion resistance, compared to metastable β alloys containing noble elements (Ti-35Nb-5Zr with α phase precipitated in β phase and Ti-35Nb-10Zr with only β phase microstructure) probably due to the much lower elastic modulus of the β alloys (10–30 GPa). The better corrosion resistance of Ti–6Al–4V ELI (low interstitial element) in the martensitic state with respect to that of Ti–13Nb–13Zr solutionized and quenched has been attributed to the higher elastic modulus of the Ti–6Al–4V alloy [36]. The Ti–6Al–4V alloy with bimodal microstructure exhibited a lower corrosion resistance with respect to the Ti–13Nb–13Zr with mainly beta matrix/alpha particles [49], while the corrosion resistance of Ti–6Al–4V ELI alloy after solutionizing and water quenching has been found higher than that of Ti–13Nb–13Zr both cold rolled and hot rolled after solutionizing and water quenching [36]. For the Ti–13Mo–7Zr–3Fe (TMZF), the corrosion resistance is improved in the solutionized and quenched state (metastable β phase) with respect to the slow cooled and aged one (β phase+ grain boundary and precipitated α phase) due to the absence of solute partitioning effect [8].

The microstructure of α + β and β titanium alloys depends on alloy composition, thermomechanical, and heat treatments. The different microstructures guarantee the mechanical properties required for biomedical application (elastic modulus, strength, fatigue, fracture toughness) and affect wear and corrosion behavior. Not always mechanical and corrosion performances match together. In this case, in order to improve the corrosion resistance of the alloy and extend the service life of implants, surface coatings need to be applied [22,50].

3. Electrochemical Corrosion of Ti Alloys in a Biological Environment: Overview

Metals and alloys' interactions with aqueous biological environments may cause damages to the metallic biomedical implants and undesired release of metal ions according to spontaneous electrochemical phenomena. In this section, a basic overview of the electrochemical corrosion processes and their occurrence in the body environment is provided.

The electrochemical corrosion processes at the surface of metal need to satisfy two essential conditions, namely, that (i) the metal is totally or partially covered by an electrolyte layer and (ii) the interface of metal–electrolyte is present in oxidated species thermodynamically liable to electrochemical reduction. As shown in Figure 4, the electrochemical process is the sum of the anodic reaction of metal oxidation and the reduction reaction of hydrogen ions and/or molecular oxygen, namely, the typical oxidated species present in a humid and aerated environment. The two half-electrochemical reactions can be schematized as follows:

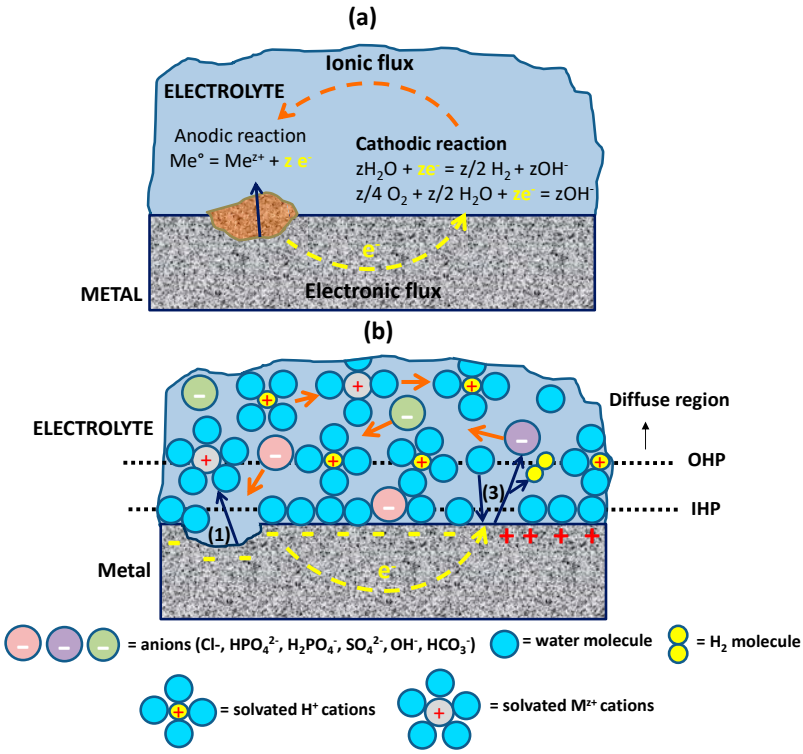

Figure 4. Scheme illustrating (**a**) the electrochemical corrosion process at a metal or alloy surface; (**b**) double-layer structure on a corroding metal showing inner (IHP) and outer (OHP) Helmholtz planes and related flux of ions (anions toward anodic areas and cations toward cathodic areas) upon polarization. Electrochemical corrosion allows the spontaneous anodic polarization of some areas and cathodic of other areas of the metal–alloy surface.

Oxidation:

$$M \rightarrow M^{z+} + ze^{-} \tag{1}$$

Reduction:

$$z/4\ O_2 + ze^{-} + z/2\ H_2O \rightarrow zOH^{-} \tag{2}$$

and/or

$$zH_2O + ze^{-} \rightarrow z/2\ H_2 + zOH^{-} \tag{3}$$

Global reaction:

$$M + z/4\ O_2 + z/2\ H_2O \rightarrow M^{z+} + 4OH^{-} \tag{4}$$

and/or

$$M + zH_2O \rightarrow M^{z+} + z/2\ H_2 + zOH^{-} \tag{5}$$

The two half-reactions occur at different areas of the metal and the closure of the electric circuit is possible due to the ionic transport through the aqueous electrolyte and the electron transport through the metallic substrate (Figure 4a). The two electrochemi-

cal reactions are independent and physically delocalized; however, their reaction rates, expressed in terms of electric current, are the same when the electrolyte solution and the alloys have a high ionic conductivity. The half reaction (1) generates an electric field and the produced metal cations need to pass through the electrical double layer toward the bulk of the solution. The double layer is generated every time metal is immersed in an aqueous solution because of the arrangement of charges at the metal surface, and it is modified upon polarization. As shown in the sketch of Figure 4b, relating to a corroding metal, electrons are accumulated in the metal anodic areas due to metal oxidation, positive charges in the metal cathodic areas where reduction takes place (Equation (2) or (3)), and excess of anions or cations that are rearranged in the solution according to charge compensation. In particular, anions are transported toward the anodic sites and cations toward the cathodic sites. The potential barrier generated across the double layer, the nature of ions, and pH strongly affect the kinetic of the process and the products formed by metal oxidation (kinetic and pH-dependence aspects relating to titanium corrosion are detailed below in the discussion of Figure 5).

Understanding if a particular metal or alloy is resistant in the body environment is essential for the design of biomedical plants and prothesis. A parameter that significantly affects the corrosion of a metal alloy is the pH of the solution. Through the use of Pourbaix diagrams [49,51], we can perform a visual inspection of the metal immunity, corrosion, and passivity fields in a potential pH plane at 25 °C, as reported in Figure 5a, for the aerated titanium–water system. The diagrams are constructed on the basis of thermodynamic chemical and electrochemical equilibrium reactions involved in the corrosion process as functions of potential and pH and are not able to provide kinetic information.

Typically, the occurrence of corrosion phenomena can be avoided by several thermodynamic or kinetic protection methods [52]. For biological implants, corrosion protection is typically realized by coating, i.e., the physical interposition of a corrosion-resistant layer between the alloy and the corrosive solution. For general applications, the coating often consists of (i) a metal chemically different from the substrate that has a sacrificial role, (ii) a metal oxide formed by oxidation of the metal–alloy substrate, or (iii) an organic compound. For the applications in the human body, corrosion protection starts from the choice of the material, which must be a biocompatible metal, or an alloy predisposed to the formation of resistant oxide layers on its surface by oxidation. Additionally, its repassivation capability in the bioenviroment where it will be implanted is fundamental. These considerations have led to extensive use of titanium and its alloys.

In the case of titanium and its alloys (and many other metals with active–passive behavior, such as Cr, Ni, and Al), a corrosion-resistant passive coating is naturally formed on their surface by oxidation of titanium in presence of the oxygen of the air. However, the oxide coating can be also induced by electrochemical and other oxidation processes to increase the thickness and modify the morphochemical properties of the layer improving corrosion resistance before implantation (see Section 4). The corrosion resistance of metal alloys, i.e., their ability to passivate and repassivate in body fluid environments, is primarily studied by recording and analyzing the polarization curves in the corrosive environment. By looking at the theoretical polarization curve E-log $|i|$ illustrated in Figure 5b and relating to a general metal or alloy with active–passive behavior in a specific solution, it can be immediately observed that the metal dissolution (corrosion), the formation of a passive metal oxi(hydroxide) coating, and its stability are strongly dependent of the electrochemical potentials at which the alloy is polarized. In fact, by increasing the polarization potential (black curve in Figure 5b) of the metal alloy, the curve E-log $|i|$ shows a linear trend in agreement with the Tafel equation. In that zone, the kinetic of the process is controlled by the charge transfer at the metal surface ($M \rightarrow M^{z+} + ze^{-}$), and the alloy is actively corroding. Proceeding with the potential increase, the current density reaches a maximum value (i_{cr}) at the Flade potential (E_{flade}) at which the metal oxide begins to form.

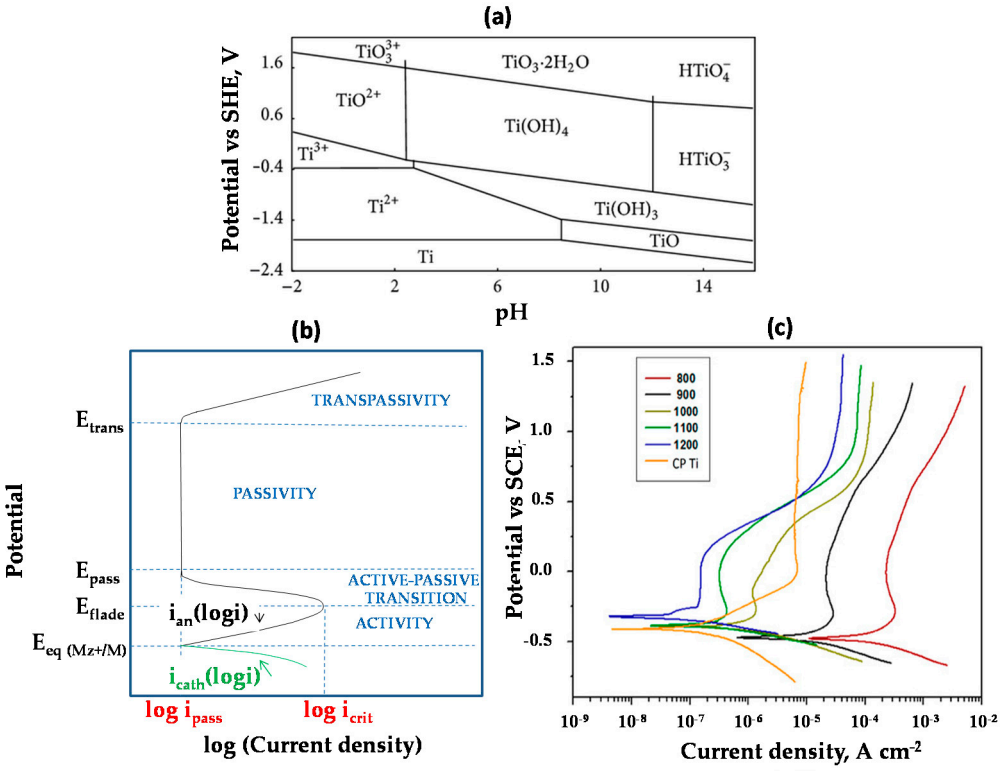

Figure 5. (**a**) Potential pH diagram for the Ti–H_2O system at 25 °C. Reproduced under the Creative Commons Attribution License from [51]. (**b**) Theoretical passivation potentiodynamic polarization curves relating to a general metal or alloy with a typical active–passive behavior in a corroding environment. E_{pass} = passivity potential, E_{flade} = Flade potential, E_{corr} = corrosion potential, E_{trans} = transpassivity potential, i_{pass} = passivity current density, i_{crit} = critic current density. (**c**) Experimental passivation potentiodynamic polarization curves relating to a Ti-20Nb-13Zr alloy processed at different consolidation temperatures in a simulated body fluid medium. Reproduced under the Creative Commons Attribution License from [53].

Then, at the passivation potential (E_{pass}), the current density drastically decreases to a minimal value (i_{pass}), and the alloy enters in the passivation zone, where a compact and corrosion-resistant oxide layer is uniformly formed at the surface, and the current density ideally remains constant to the passivation value (i_{pass}). In the case of titanium, different crystalline and oxidation forms of titanium oxide (amorphous, rutile, anatase) can be formed in the passivation zone depending on the applied potential and temperature, as illustrated in Figure 6. In the same Figure, we can also observe the different corrosion phenomena caused by potential increases or decreases and by temperature treatments in acidic conditions. By increasing temperature over 70 °C, rutile formation is favored within a certain threshold. After that breakdown takes place and the oxide film is broken in some areas where a local thickening occurs, the process of localized corrosion begins in these points, bringing about the crevice corrosion phenomena. Similarly, at room temperature, a severe increase of potential causes a similar effect that produces pitting corrosion.

The presence of a coating on the metal alloy surface decreases the kinetics of the electrochemical reactions to insignificant values of the corrosion current density. Of course, physicochemical and morphological features of the coating have an essential role in determining the corrosion resistance in the selected biological environment. The role played by the coating can be more complex than a simple inert physical separation between the two "reagents" (metal and electrolytic solution). The nature of the metal alloy is usually selected according to its capacity to form passivation film in the aggressive solution.

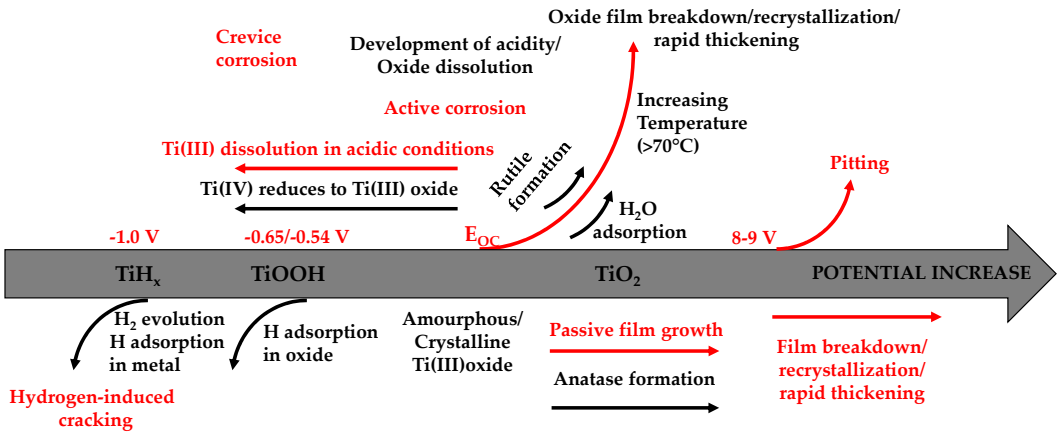

Figure 6. Scheme showing the properties of the passive film on titanium as a function of potential and temperature. E_{OC} = open circuit potential. Adapted from [54], copyright (2017), with permission from Elsevier.

Of course, the shape of the passivation curve and the values of the characteristic potentials and currents change with the environmental conditions (pH, anions nature and concentrations, temperature, and microorganisms). For example, Figure 5c reports the effect of the consolidation temperature on the passivation curves relating to a Ti-20Nb-13Zr alloy in a simulated body fluid medium [53].

The polarization of the alloy at relevant potentials able to grow highly resistant oxide coatings can be performed before implantation by electrochemical growth (see Section 4 for alternative methods) of highly performant oxides in relevant electrolytes. However, the ability of the body fluid to provide the right repassivation conditions that bring the alloy to the passivity thermodynamic and kinetic existence field is crucial. The capability of the biological environment to repassivate the alloy is fundamental to repair possible damages provided by localized corrosion effects during implantation. In fact, during the corrosion process (active state), the metal can protect itself by repassivation. Protective metal oxides can electrochemically form on the metal surface if the coupled cathodic process (O_2 or H^+ reduction) generates a corrosion potential higher than the equilibrium potential of the anodic reaction of oxide formation. Therefore, the composition of the solution is crucial for corrosion resistance and repassivation processes, and the most important parameters to be monitored are pH and halogen concentration.

In the human body, the water content can be up to 60% of its total mass. The body fluids can be intracellular or extracellular, such as blood, lymph, cavities, and channels of the brain and spinal cord and body tissues. They can be intracellular (about 70%) and extracellular fluid (about 30%). Body fluids contain many electrolytes, such as H^+, Na^+, K^+, Ca^{2+} and Mg^{2+}cations, and OH^-, HCO_3^-, Cl^-, PO_4^{3-}, and SO_4^{2-} anions. Their presence greatly affects the cell membrane potentials and osmolarity of body fluids, determining the goodness of many bodily functionalities such as metabolism. The normal temperature of body fluid is 37 °C. Therefore, biomedical implants should be designed by considering their possible corrosion at this temperature for all their time of functioning.

Corrosion events can have a general or localized extension on the surface of the alloy. In the first case, the electrochemical reactions interest the whole surface of the metal in a uniform way, generating a slow and constant corrosion rate that does not affect the performance of the alloys. In the second case, the distribution of the anodic and cathodic areas and their rate are not uniform: at some points, the metal oxidizes very quickly, producing significant damages along with the alloy dept (pitting). It mainly occurs in presence of chloride ions.

Electrochemical corrosion, coupled with mechanical stress, can produce scratching, weakening, and cracking of the components of the biomedical implant [55]. These types of corrosion are shown in Figure 7 for titanium implants in the oral cavity. Galvanic corrosion and pitting are, in general, the most common; nevertheless, fretting and wear

are specifically involved in Ti-6Al-4V alloys [56]. Localized corrosion principally occurs at connections of modular joint replacement components [57] and when galvanic couples are formed, for example, Ti and Ti-6Al-4V alloy [58].

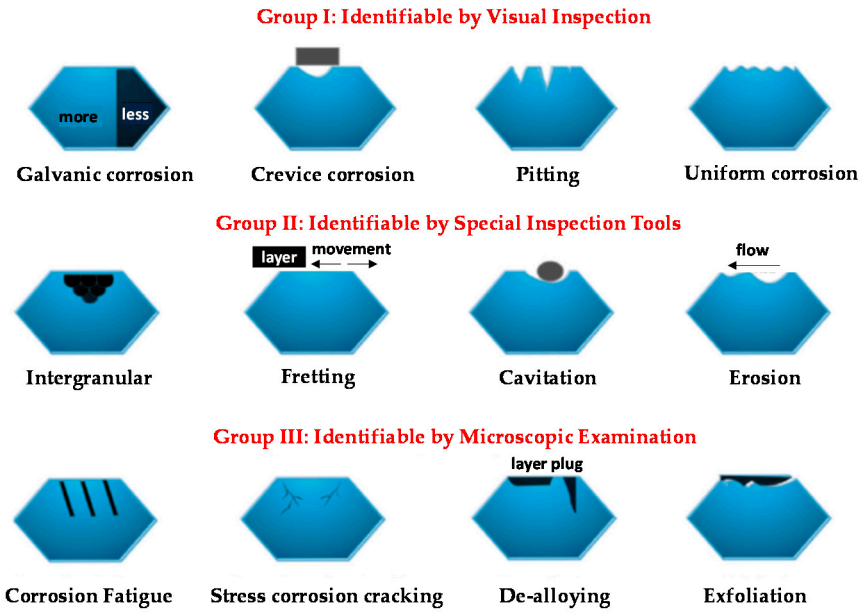

Figure 7. Corrosion forms in titanium-based dental implants are classified into three groups according to the necessary identification technique. Adapted under the Creative Commons Attribution License from [59].

There is a body of work on the corrosion of biomedical implants. For further details, refer to the numerous reviews reported in the literature [60–66] and references therein.

In the following sections, we specifically discuss the techniques used to modify the surfaces of Ti-6Al-4V and beta-Ti alloys by growing a passive oxide coating (Section 4) and the most important literature results showing the corrosion resistance of such passive films in bioenvironments (Section 5).

4. Passive Layers on Biomedical Ti-6Al-4V and β-Ti Alloys

The biocompatibility and durability of biomedical Ti alloys strictly depend on the microstructure, chemical composition, and mechanical strength of the surface coating [5]. The surface treatment of Ti alloys before implantation is a crucial step to improve the corrosion and wear resistance and the biofunctionality of the resulting coating. Several techniques can be applied to obtain biocompatible and corrosion-resistant coatings on Ti alloys. In this review, we focus on improvements in the corrosion resistance properties of the passive coatings considering that also the other two requirements (biocompatibility and wear resistance) must be satisfied at the same time. In fact, in some cases, the procedures carried out to grow more or less corrosion-resistant titanium oxide coatings on the alloy are simultaneously finalized to improve the titanium ability to induce apatite formation on its surface in simulated body fluid (SBF) [67]. In fact, titanium oxide is biologically inactive and the presence of hydroxyapatite on the surface favors the osseointegration of the implant, which is extremely important, especially in orthopedic applications.

4.1. Electrochemical Passivation

In natural conditions, titanium is covered by a native oxide film of some nanometers [68], which can be increased by electrochemical anodization at a rate of about 2–3 nm V^{-1} [69–73].

Electrochemical passivation of Ti alloy by anodization (Figure 8A,B) is one of the most useful and extensively studied processes [74] to increase the thickness and improve the morphology (compact oxide or nanotubes arrays, Figure 8) of the passive layer [75].

The electrochemical technique is a low-cost and rapid technique, allowing an easy growth of the passive layer on the metal surface and precise control of its thickness, composition, morphology, and general properties by means of a simple regulation of the electric process parameters and electrolyte composition and pretreatments of the electrode surface [76–79]. Many research studies are focused on the research of the best electrochemical parameters for obtaining Ti alloys' passive layers with the right thickness, morphology, corrosion stability, and bioactivity for biomedical application [80,81].

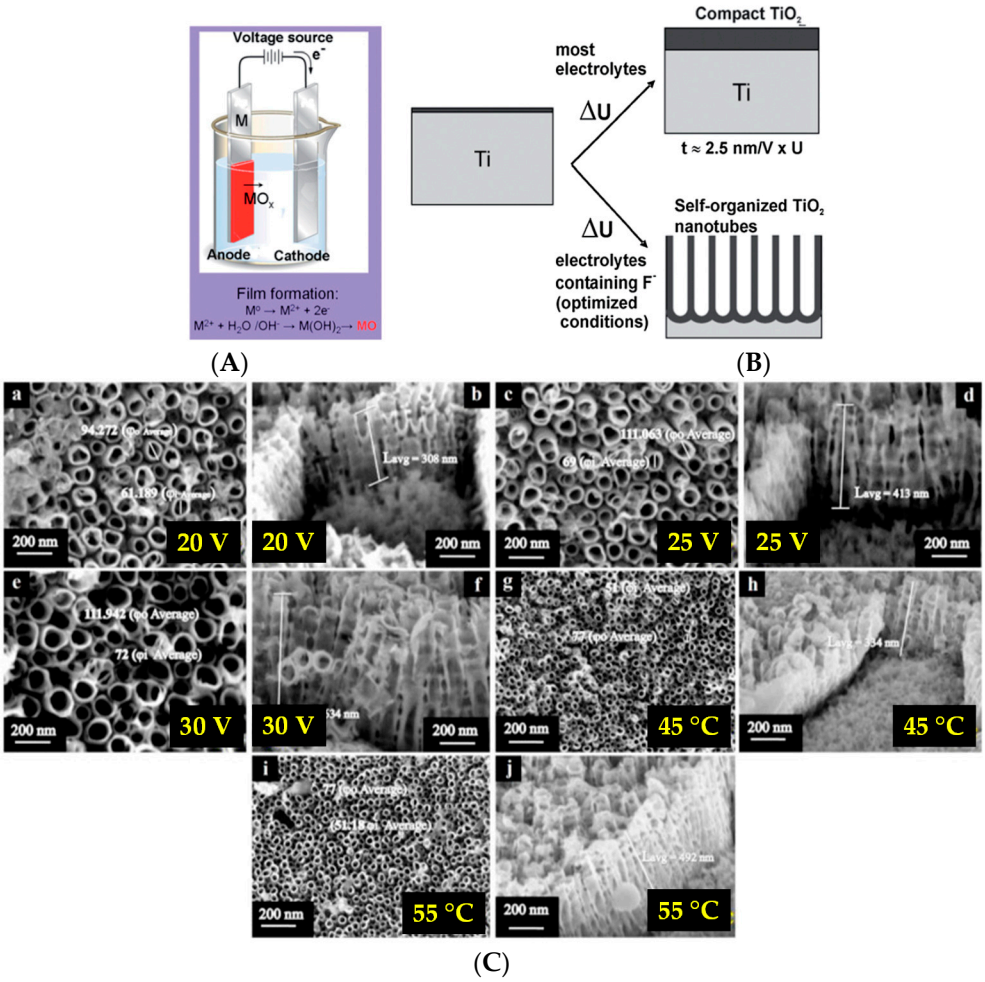

Figure 8. (**A**) Scheme illustrating the anodizing setup used to grow passive Ti oxide layers on Ti or Ti alloys. (**B**) A barrier layer or porous nanotubular layer can be obtained depending on the electrolyte's nature. Reprinted from [82], copyright (2007), with permission from Elsevier. (**C**) FE-SEM micrographs of NTs diameter and length on Ti–6Al–4V at (**a**,**b**) 20 V, (**c**,**d**) 25 V, (**e**,**f**) 30 V at 30 °C, (**g**,**h**) 20 V at 45 °C, and (**i**,**j**) 20 V at 55 °C. Reprinted from [83], copyright (2020), with permission from Elsevier.

Anodic nanotubular titania coatings (Figure 8B,C) are of great recent interest for biomedical applications [84] due to many advantages, namely, (i) they increase adhesion and functionality of the osteoblast cell [85], (ii) they favor the hydroxyapatite formation [86] and tissue integration [87], and (iii) they improve cellular interactions because of the high surface area available for protein adsorption and antibacterial agents [88]. In addition, the strong bond between the coating and metal characteristic of electrochemical anodization protects the oxide film from delamination processes [29]. Shape, diameters, and thicknesses of titania nanotubes coatings grown by electrochemical oxidation can be widely tuned by regulating the concentration of the electrolyte, type of solvent, and electrolyte, anodizing electrical conditions, as shown in Figure 8C (detailed information relating to Ti-6Al-4V

and β-Ti alloys can be found in Refs. [89,90]). In general, the composition of the formed anodic oxide layer is consistent with the alloy composition and alloying elements ratio [91]; however, more details on these aspects can be found in [84] and references therein.

Modeling of nanotubular structure, diameter, and length can be developed based on oxidation parameters and the environment. The research history on this topic can be divided into generations characterized by the use of different solutions of anodization. In the first generation, the nanotubular titanium oxide layer was obtained using HF, in the second, electrolytes consisting of NH_4F and NaF. The third-generation nanotubes were developed in electrolytes based on glycol, changing the geometry of nanotubes in hexagonal. In some cases, chloride electrolytes produce an anodized called rapid breakdown anodization (RBA) with thinner nanotubes, which does not require too much time, making it an easy option [92].

The corrosion resistance of Ti alloys coated by a nanotubular layer of titania is mainly related to the barrier layer located at the bottom of the porous structure in direct contact with the metal [93,94] where the titanium oxide is thermodynamically more stable and protective against metal ions dissolution (Figure 8B).

4.2. Thermal Oxidation

Coatings of high corrosion-resistant biomedical titanium oxide can also be obtained by thermal oxidation. The morphology of these oxides is typically porous, and the thickness is quite high, in the order of 10–20 μm [95]. The mechanical and chemical stability, thickness, and crystallinity of oxide layers grown by thermal oxidation on Ti and Ti alloys are strictly dependent on the process temperatures (higher than 200 °C), time, and mode of cooling. Higher temperatures and longer times generally strongly increase the hardness and roughness of the oxide layers in both CP-Ti and Ti alloys. Additionally, fast cooling decreases the adhesive strength, friction characteristics, and wear and fatigue resistance [96].

TiO_2 anatase is converted into rutile, which possesses a lower capability to release ions [22] and greater biocompatibility [97]. In order to decrease the longtime of alloy processing and equipment costs of this method, a novel fabrication process in which thermal oxidation, cutting, and surface modification are integrated has been recently developed [98].

4.3. Plasma Electrolytic Oxidation

Plasma electrolytic oxidation (PEO), also named micro-arc oxidation (MAO), occurs when a metal is electrochemically anodized at high applied voltages at which micro-arc phenomena can take place. These phenomena occur in the transpassivation region of Figure 5b, in which the current density notably increases, becoming responsible for the dielectric breakdown of the TiO_2 passive layer. At the breakdown voltage, the metal surface is exposed to the solution at some points where the hydroxide ions react with Ti ions very rapidly to grow again the titanium passive film and repair the passive coating. This technique is interesting because the newly formed titania passive layer has many advantageous features, namely, (i) it has a porous structure strongly adherent to the metal that enhances the biological activity and (ii) its surface has Ti-OH functional groups and oxygen vacancies that can improve the biological and antibacterial ability, respectively [99]. In this case, the method is also reported as "ion implantation". In addition, the PEO process provides the opportunity to incorporate calcium and phosphorus ions into the oxide layer by opportunely regulating the composition and concentration of the electrolyte. The incorporated Ca and P ions were even crystallized into hydroxyapatite or other calcium phosphates by a hydrothermal treatment. Proper selection and combination of composition and temperature of the electrolyte, alloy composition, voltage, current density, time of deposition are necessary to obtain corrosion resistance and biofunctionality at the same time in a single process [100,101].

For example, the use of high potentials improves on the one hand, the Ca and P ions incorporation into the coating promoting the formation of apatite [97], and on the other hand, it deprives the coating compactness by generating porosity, cracks, and inadequate

adhesion. The last effect favors implant corrosion because corrosive ions can easily reach the inner thin barrier layer underlying the porous structure where the attack is facilitated.

Pretreatments of the alloy by anodization in relevant electrolyte before PEO can also be performed to improve the corrosion resistance of the inner layer by increasing its thickness and/or its density.

5. Electrochemical Biocorrosion of Passive Coatings on Ti-6Al-4V and β-Ti Alloys

5.1. Methods

Results obtained by Web of Science, PubMed, and Science Direct databases were used to select relevant papers for Sections 5.4 and 5.5 according to different keywords coupling (i) biomedical AND beta-titanium AND corrosion, (ii) biomedical AND Ti-6Al-4 V AND corrosion, (iii) beta-titanium AND biocorrosion AND passive film, and (iv) Ti-6Al-4 V AND biocorrosion AND passive film. After reading the abstract of the found products, research papers reporting data on electrochemical corrosion of titanium alloy in simulated body fluid and passive layer formation were selected, while papers that did not report electrochemical polarization curves or corrosion mechanisms were excluded.

5.2. Overview

The passive film formed on the surface of titanium alloys occurs when it is exposed to oxygen, air, or some aqueous solution; this layer has a thickness of nanometers and it can be easily damaged [102,103], but that damage can be reestablished by itself in presence of oxidant conditions [104].

The surface of the material provides very important properties to cell differentiation, maturation with osteogenic capacity, and ensuring the adherence of cell implant. The production of TiO_2 layer on the surface material occurs also when titanium alloys are immersed in body fluids although some surface treatments have been developed, e.g., plasma electrolytic oxidation or anodized, to create TiO_2 layers with specific properties such as adherence and compactness [105].

The chemical composition of oxides grown on Ti-6Al-4V or β-Ti alloys is directly correlated with the osteointegration process and the retard of itself due to the number of metal ions (Ti, Zr, Al, V, Nb, etc.) those could create interference by a cytokine osteolytic [106,107]. The purpose of surface modification in Ti alloys is to maximize bioactivity; when exposed to natural tissue, providing surface treatment could provide better osseointegration and bioactivity, with the latter avoiding bacterial adhesion on implant surface [108].

Taking into account that corrosion behavior is one of the most important challenges for biostability and biocompatibility, the electrochemical behavior of passive layers will depend on the electrolyte; for this reason, it is necessary to characterize Ti alloys with surface treatments in physiological environments because, in those type of alloys, a high corrosion resistance implies that metal ions will not be introduced in the bloodstream [82,109].

5.3. Biochemical Environments Encouraging Ti-Alloy Passive Layer Corrosion

As highlighted in a recent review, the impact of corrosion products on implant durability and human healthiness is strictly dependent on the biological environment [7,110]. The presence of some chemical compounds, such as strong acids or chloride and fluoride, or bacteria that produce organic acids can irremediably attack the oxide layer of the titanium-based implant, beginning the corrosion process. For example, rubbing with several high concentrated acids causes damages to the Ti-6Al-4V surface, as observed by Wheelis et al. [111]. At low pH, the presence of halogens increases the risk of corrosion because of the incorporation of such anions in the passive film formed in the biological solution. Titanium grade II or IV immersed in saliva containing fluoride ions shows pitting corrosion with several patterns [112]. On the contrary, the Ti-6Al-4V alloy exhibits generalized and thus slower and safe corrosion. The biological environment should not combine high acidity and high fluoride content to guarantee a low corrosion rate. For pure titanium, the maximum range value of sodium fluoride has been identified to be about 200–9000 ppm,

corresponding to a pH of 3.5–7.0 [113]. Additionally, the surface metallurgy of titanium is demonstrated to be more influenced by 35% hydrogen peroxide than 16% carbamide peroxide [114]. Another interesting result is the ability of albumin and H_2O_2, both of which are contained in a peri-implant environment, to increase the corrosion rate of titanium grade IV at human body pH and temperature conditions [115]. Often, the concentration of a corroding species is fundamental in determining the corrosion phenomena; for example, Ti-6Al-V disks result in being locally attacked by 0.2% chlorhexidine digluconate, while they are immune at lower concentrations. Additionally, the electrochemical potential of the alloy can be affected by the presence of bacteria favoring corrosion. In this case, the release of titanium can be visually observed by a dark tissue discoloration in tissues adjacent to medical implants [116].

5.4. Electrochemical Biocorrosion of Passive Coatings on Ti-6Al-4V

As discussed in detail in previous sections, passive coatings are naturally formed in the body fluid or pre-formed by relevant surface treatments on the titanium alloy surface (Section 4). In this section, we report the main results concerning the electrochemical biocorrosion of passive coatings on Ti-6Al-4V alloys with and without the preliminary growth of a thick oxide layer on their surface by analyzing the factors controlling the corrosion process.

In the work of Alves et al. [117], it is proved that the solution temperature and immersion time are key factors in regulating the corrosion resistance of Ti-6Al-4V alloys. The electrochemical results show that at 25 °C Ti-6Al-4V and Ti-6Al-4V ELI are superior with respect to Ti CP4 in terms of corrosion resistance. In fact, E_{corr} and i_{corr} recorded in Hank's solution show that Al and V alloying elements reduce the dissolution rate of the passive layer formed in the solution. On the contrary, at 37 °C (human body temperature value), the results are inverted, and the passive film on Ti-6Al-4V becomes less resistant than that of titanium due to local corrosion processes accelerated by the presence of chloride ions in Hank solution. Both vanadium [117] and aluminum ions can be found in the electrolyte [42,118]. Additionally, the effect of immersion time is to shift E_{corr} to more positive values, located in the passivation zone at both temperatures. This result indicates the growth of a protective passive layer on the alloy surface during the immersion time. Both alloys show a large passivation range in the potential vs. log i current density plot after 5 min of immersion (Figure 5b). The formation of oxide layers on TiCP4 and Ti-6Al-4V after immersion in simulated body fluid (SBF) is proved by the electrochemical impedance spectroscopy (EIS) technique [117]. EIS spectra relating to Ti-6Al-4V in SBF show one time constant at 25 °C indicative of a single oxide barrier layer, while at 37 °C, the spectra show two time constants attributed to the formation of a passive layer constituted by a compact inner barrier and a porous outer layer [117], composed essentially of titanium oxide (TiO_2) with a composition transient region between the two layers [119]. The effect of temperature and time of immersion in the SBF solution on the morphology and thickness of the passive layer grown on titanium and Ti–6Al–4V alloy is schematized in Figure 10. In the sketch of Figure 10c, the principle of NTs formation is reported. The growth of the double structure proceeds according to three stages: (i) first, a compact oxide layer grows on metal surface in contact with an electrolyte, (ii) then, the initiation of pores or a slight pitting process on the oxide layer occurs, and (iii) finally, NTs arrays from pits or pores are formed.

The EIS technique possesses the ability to reveal the morphology and corrosion resistance of the layer showing in the Nyquist plot two separated arcs, i.e., time constants, corresponding to the outer layer (porous or NTs layer) at high frequencies and the inner layer at low frequencies. This event is known as the double-layer effect. The revelation of pores o NTs through an in situ technique is important because the morphology quality (distribution of nanotubes/pores uniformity) modifies the electrochemical parameters of corrosion. The number of time constants detected in EIS experiments depends also on solution temperature. Some authors report that at 25 °C EIS analysis shows only one time constants, while at 37 °C, the double-layer effect appears [120–123]. The presence of a

constant phase element (CPE) element in the circuit used to fit the experimental EIS plots describes a process of nonuniform current distribution or a possible dispersion of time constants on electrode surface [124–126]. This effect can also occur due to the difference in phase of Ti-6Al-4V alloy since NTs are not uniform, being porous in the beta phase and nanotubular in the alpha phase [126]. Orazem and Tribollet [124] characterized Ti-6Al-4V using EIS and showed a double-layer structure that increases corrosion resistance when it is treated at the surface. In this study, the authors conclude that for a better protective layer, it is necessary to increase the percentage of oxygen and to decrease that of nitrogen.

The influence of the alloy composition and microstructure on the corrosion resistance of Ti6-Al-4V has been also evaluated [127]. Potentiodynamic analysis reveals that i_{corr} decreases using Ti-6Al-4V and Ti6Al4V-ELI alloys instead of pure titanium in phosphate-buffered solution (PBS) with and without the addition of bovine serum albumin (BSA). The introduction of Al and V in the titanium metal is beneficial toward the active and passive dissolution of titanium and significantly reduces the wear accelerated corrosion under tribocorrosion conditions. Ti-6Al-4V alloy with α+β phase microstructure shows a wear resistance strongly higher than that of the Ti Grade 2 α phase microstructure under normal load of 5 N and sliding speed of 20 mm/s. The effect of BSA is quantified in a negligible increase of corrosion current density for Ti-6Al-4V and Ti-6Al-4V ELI alloys and a decrease for pure Ti (Grade 2 and Grade 5). Mainly, the addition of BSA increases the passivation current for both the materials with respect to the pristine PBS solution.

The corrosion resistance of Ti-6Al-4V alloy has been also studied after coating by an oxide layer grown by PEO [128]. The electrochemical behavior of the coated alloys was studied by potentiodynamic polarization, and the results showed that coated samples have corrosion potentials more positive than uncoated titanium. The measured corrosion current density of PEO coated titanium is lower than uncoated Ti with values of 121.58 nA/cm^2 against 494.5 nA/cm^2, meaning that corrosion kinetic is slower in coated titanium. Therefore, as shown in Figure 9, the E_{corr} of coated titanium is higher than the uncoated sample, meaning that coated samples need more energy to begin the corrosion process [128].

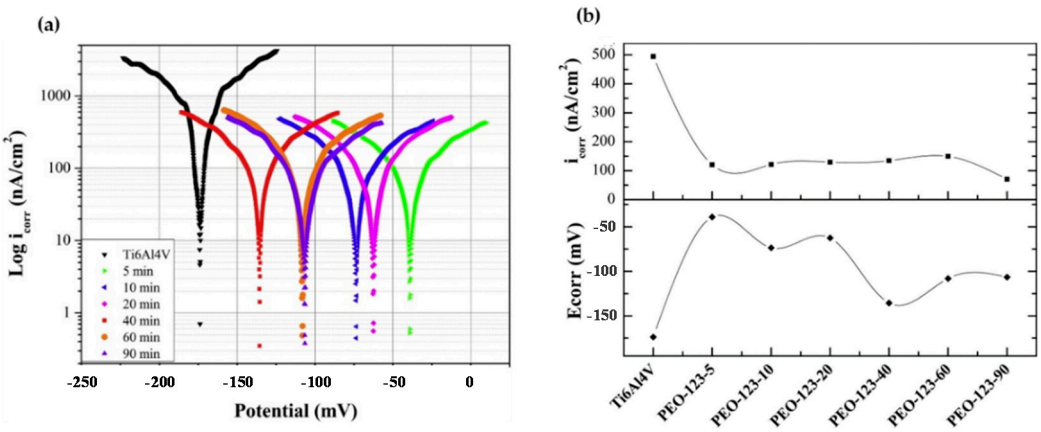

Figure 9. (**a**) The electrochemical polarization curves recorded in SBF solution at 36.5 °C for the PEO coatings at different deposition times and uncoated Ti-6Al-4V alloy. (**b**) The variations of the electrochemical parameters of uncoated Ti-6Al-4V alloy and the PEO coatings at different deposition times. (**a**,**b**) Reprinted from [128], copyright (2016), with permission from Elsevier.

A two-step plasma electrolytic oxidation (hybrid PEO coating) with alkali treatment (AT) has also been investigated for bioactive and biocorrosion-resistant alloys. Nabavi et al. [123], in 2019, studied the effect of this technique on the biocorrosion resistance of Ti-6Al-4V (grade 5) and CP-Ti (grade 1) substrates. The first step of PEO in a mixture of trisodium orthophosphate and sodium citrate solution aims to improve corrosion resistance, while the second step of PEO is performed in calcium acetate and sodium phosphinate monohydrate solution to increase bioactivity due to the incorporation of calcium and phosphor in the

protective layer. The alloys were subjected to structural, morphological, and electrochemical characterizations. The electrochemical results in the SBF solution are mainly correlated to the ability of the second PEO step to grow a compact layer. Potentiodynamic polarization and morphological results showed that the corrosion current density strongly depends on the morphology and compactness of the coating. Samples subjected to long times of PEO show large pores that facilitate the penetration of ions, and the passivation range is reduced. EIS analysis reveals a double-layer structure known to exhibit two-time constants in the Nyquist plot [129,130] in which the inner layer dominates the low-frequency range, and the outer and porous layer describes the high frequencies. When the author used a hybrid PEO coating, a three-time-constant behavior appears, showing the presence of another outer porous layer. This behavior is represented in Figure 11, with typical Randle circuits accepted in the literature [123]. For this reason, it is convenient to seal NTs when a PEO is applied. Further, X-ray photoelectron spectroscopy (XPS) and Fourier transform infrared spectroscopy (FTIR) analyses corroborate the surface formation of hydroxyl groups and their involvement in the bioactivity improvement of the alloy.

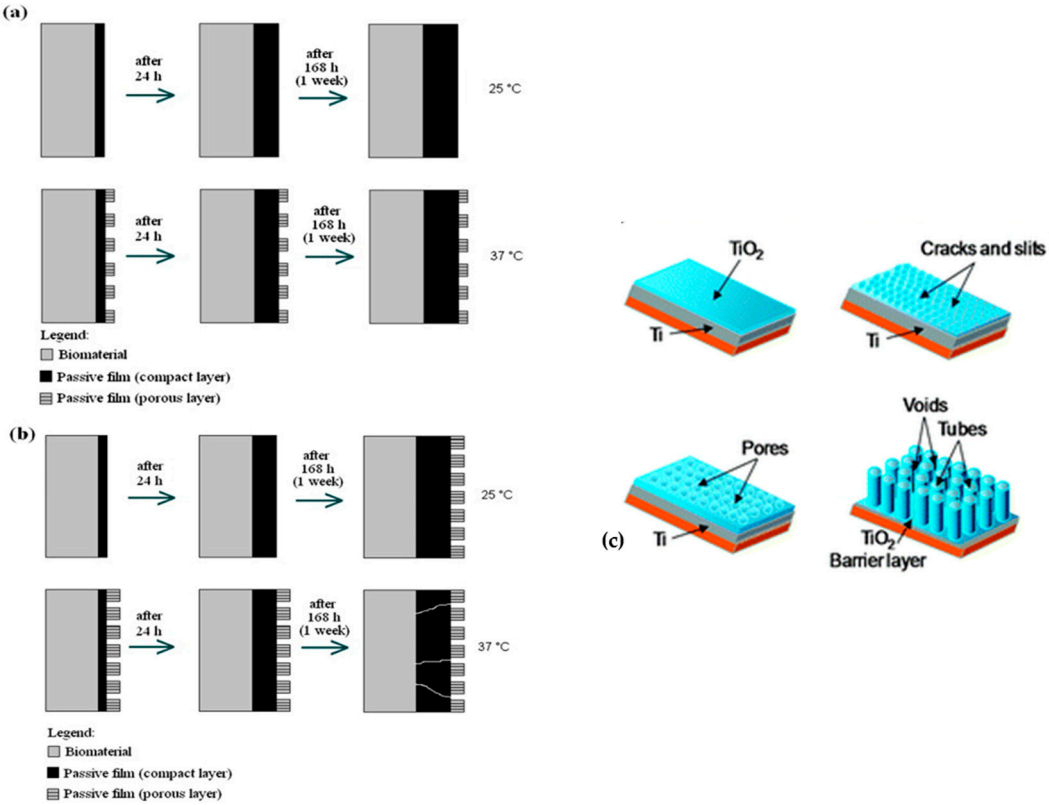

Figure 10. (**a**,**b**) Scheme showing the effect of solution temperature and time of immersion in SBF on the formation of a passive layer on (**a**) Ti and (**b**) Ti–6Al–4V alloy. Reprinted from [117], copyright (2009), with permission from Elsevier. (**c**) Growth of a nanotubes array on titanium metal. Republished with permission of Royal Society of Chemistry from [120]; permission conveyed through Copyright Clearance Center, Inc. Improved Figure.

Lario et al. [131] studied the effect of nanotopography and annealing on the corrosion resistance of the Ti-6Al-4V ELI alloy. Different TiO_2 surfaces and nanotubes have been coated on Ti-6Al-4V ELI by electrochemical anodization and the electrochemical corrosion resistance investigated in 1 M NaCl solution. TiO_2 nanotubes arrays show better corrosion resistance than the native oxide layer due to the higher surface area and amorphous crystal structure. TiO_2 nanotubes thermal treatment has the effect to remove fluoride ions that favor localized corrosion and stabilize the anatase phase. The corrosion potential measured by potentiodynamic polarization has a lower value for anodized than bare Ti alloy. EIS results confirm that anodic anodization of Ti-6Al-4V ELI alloy permits the growth of a

thick oxide compact layer at the base of the nanotubes array (see Scheme of Figure 8b), guaranteeing high corrosion resistance [131].

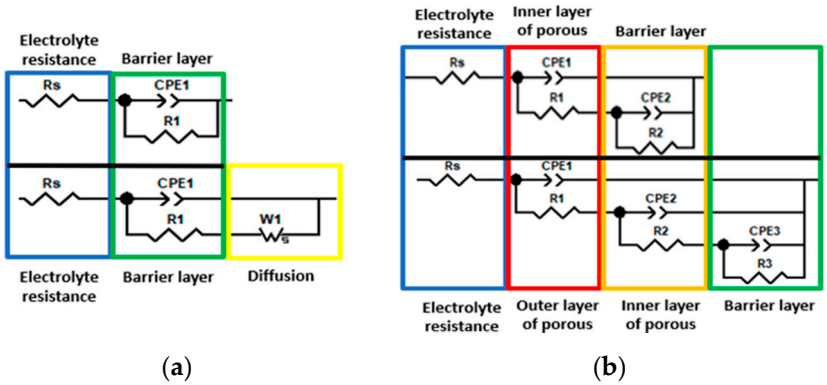

Figure 11. Equivalent Randle circuits used for the interpretation of EIS spectra recorded on Ti6-Al-4V alloy (**a**) uncoated (**b**) coated by (up) PEO (down) hybrid PEO.

The research trend to increase the corrosion resistance of Ti-6Al-4V alloy goes toward the fabrication of uniform and highly ordered nanoporous layer by anodic oxidation. In fact, this technique allows the self-organizing of the porous and nanotubes arrays on the alloy and the obtainment of a highly ordered structure by relevant regulation of the anodization parameters, electrolyte nature, and concentration, surface treatments. By reducing the defects of the porous layer, corrosion can be firmly decelerated. In a very recent study [132], electrochemical anodization has been employed to produce uniform self-organized nanoporous oxide layers (with pore average diameter of 90 nm) on the Ti-6Al-4V surfaces in ethylene glycol electrolyte containing ammonium fluoride and lactic acid. Corrosion resistance evaluated in NaCl medium strongly increases, compared to the bare Ti-6Al-4V specimen, and a further improvement is recorded after thermal annealing. In Figure 12, the ordered porous morphology (panel a) and the corresponding great increase in corrosion potential (panel b) can be observed.

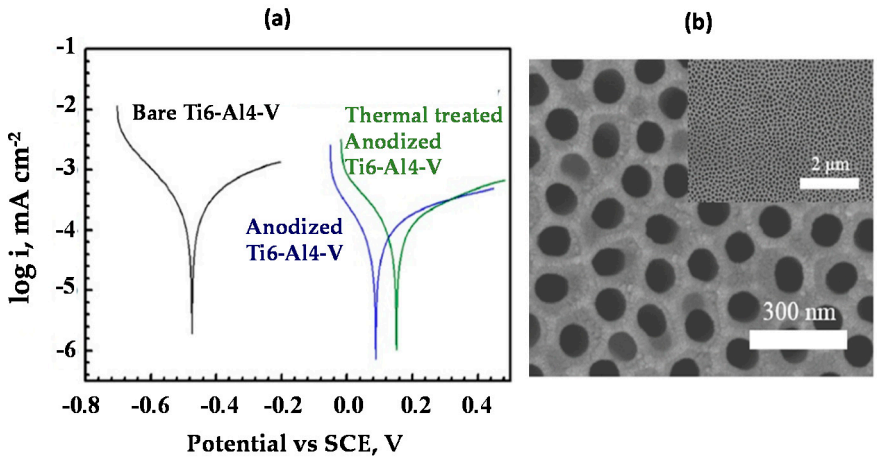

Figure 12. (**a**) Evans's diagram of three Ti-6Al-4V samples in 8 g/l NaCl solution. (**b**) FE-SEM micrograph of a nanoporous oxide grown on Ti-6Al-4V at 100 V in ethylene glycol electrolytes, NH_4F, H_2O, and lactic acid for 10 min. Reprinted from [132], copyright (2021), with permission from Elsevier.

5.5. Electrochemical Biocorrosion of Passive Coatings on β-Ti Alloys

In a very recent review [9], the corrosion electrochemical properties of uncoated beta titanium alloys have been compared to uncoated Ti-6Al-4V. The results collected in the literature are referred to the uncoated state and showed good stability and corrosion protection

for Ti-6Al-4V and beta-alloys. The good corrosion protection has been correlated to the properties of the oxide layer formed in situ in the biological environment, in particular, the presence of niobium, tantalum, and zirconium oxides in beta-Ti alloys and the modulus of elasticity and the good adherence of the oxide in Ti-6Al-4V alloys. Therefore, it is expected that a high-quality film opportunely grown on the alloy surface could transform the beta-titanium alloys into the best option to reach a biocompatible goal. To achieve this aim, the following relevant literature results of the last years on beta-Ti alloys coated by a protective oxide before corrosion experiments are discussed. Beta-Ti alloys promise challenges because of the nontoxic elements and the benefits to human osteoblasts [133]; for this reason, it is of great importance to understand how the growth of an oxide coating before or during implantation can improve corrosion resistance in bioenvironmental solutions.

It is well accepted that the addition of Nb metal enhances the passive behavior of titanium because Nb covers the anion vacancies in the titanium oxide crystal lattice [134]. The passive film constituted by Ta_2O_5 and Nb_2O_5 has more stability and high corrosion resistance in comparison to conventional Ti-6Al-4V alloys. Additionally, NbTaTi alloys possess a lower modulus than titanium due to the presence of β phase [135]. Thus, most of the β-Ti alloys' studies are focused on the development of β-Ti alloy by the addition of Nb, Ta, Mo, Fe, and other alloying metals able to confer relevant properties to the material.

With the aim to discuss the mechanism of active corrosion of bare TiTaNb alloys in SBF, we report a recent study [136] in which TiTaNb medium entropy alloys (MEA) films are proposed as a promising coating material for biomedical applications. The results show mechanical and biocorrosion resistance superior to Ti-6Al-4V alloys. The active corrosion current density in SBF recorded by polarization curves is highly lower than Ti-6Al-4V, as confirmed by EIS analysis that shows the highest insulating, capacitive, and charge-transfer-resistance parameters. In addition, TiTaNb MEA films have higher hardness, higher wear resistance, and greater biocompatibility. The mechanism of corrosion and formation of a protective film in SBF is schematized in Figure 13 and supported by XPS results.

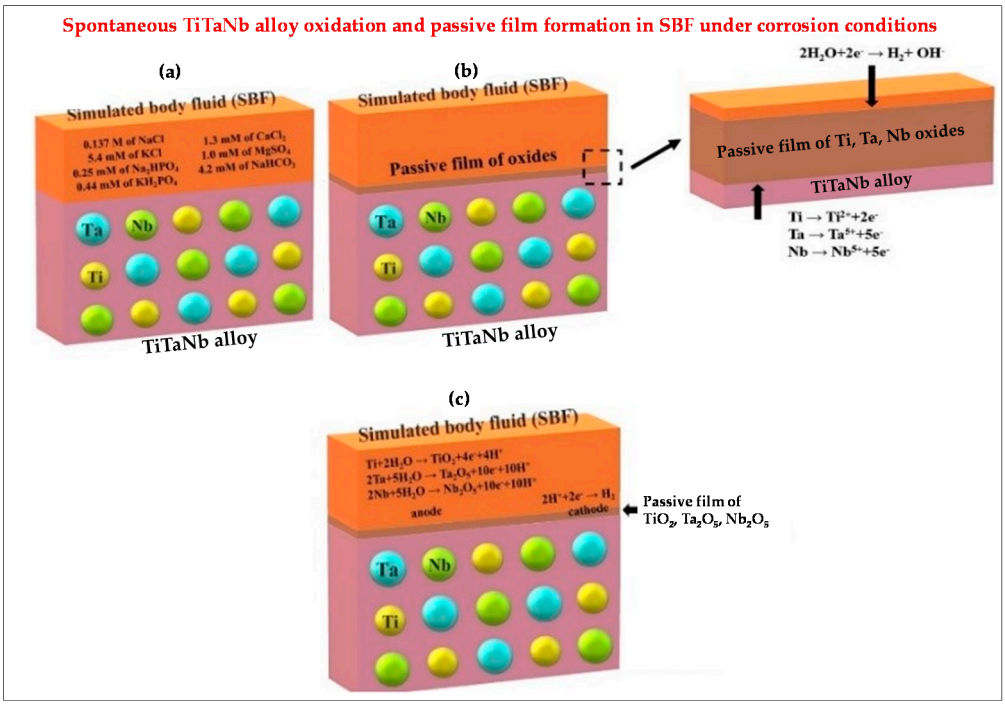

Figure 13. Spontaneous formation of a passive film on β-TiTaNb alloy under corrosion conditions: (**a**) the alloy is in contact with corrosive SBF solution, (**b**) a passive layer grows on the alloy surface under corrosion due to Ti, Ta, Nb metals dissolution and subsequent formation of the correspondent metal oxides, and (**c**) in steady state, passive layer is continuously renewed under corrosion conditions. Adapted from [136], copyright (2020), with permission from Elsevier.

The bare Ti alloy undergoes active corrosion soon after immersion in SBF by injections of Ti^{2+}, $Ta^{5+,}$ and Nb^{5+} ions in the solution, and simultaneously, the associated cathodic reduction of water with the production of hydroxyl groups occurs (panels b, c). The local increase of pH suddenly induces the formation of intermediate metal hydroxides that are then converted into oxides (reactions in panel b). After that, the formation of sites of nucleation converts into the growth of a passive oxide layer that at the end of the process reaches a thickness of about 6 nm (panel d). Another study directly compares the corrosion behavior of bare Ti–6Al–7Nb and Ti–6Al–4V ELI alloys in SBF solution [122]. Ti–6Al–7Nb alloy exhibits slower corrosion kinetics than Ti–6Al–4V ELI due to the presence of Nb that improves the oxide stability on the surface. By EIS analysis it can be concluded that for short times of immersion, a barrier layer is formed for both alloys. On the contrary, a double porous layer oxide is formed for long immersion times in SBF solution.

Stated these results, further improvements can be surely obtained by performing on β-Ti alloys a passive treatment before implantation aimed to increase the thickness and the stability of the coating. Many papers are reported on the anodic growth of nanotubular coating of beta alloys of Ti binary and Ti ternary [137,138], Ti-Nb [139,140], Ti-Ta-Zr [141], and Ti-Nb-Zr [142], TiNbTa [143], and TiNbTaZr [144]. Navarro Laboulais et al. [145] studied a novel β-Ti alloy (Ti35Nb10Ta-xFe) and the effect of iron concentration in the alloy and anodizing parameters on the passivation kinetic. As expected for barrier film anodic growth [146], the passive film thickness is directly proportional to the applied potential with a growth rate of 2–4 nm V^{-1}. The microstructure of the alloy is confirmed to be mainly composed by β phase, and the residual α phase reduces as the Fe content increases. A rise in Fe amount also affects (i) the porosity of the alloy showing pores sizes in the range of the iron powder used in the sintering process, (ii) the growth rate of the passive film, which decreases due to a higher energy barrier for ionic conduction in the oxide, and (iii) the mechanical resistance with elastic module near to the bone. Thus, the addition of iron to β-Ti alloys is promising in low aggressive environments when the mechanical resistance is crucial.

The corrosion protection of Ti alloys can be improved by coating the alloy with thick oxide layers before implantation. The thickness can be improved by anodizing the alloy in relevant aggressive solutions able to partially solubilize the oxide allowing the formation of a porous nanotubular structure, that, as stated in Section 4, also favors the biological interactions with the solution with good osseointegration [147,148]. Some studies indicate that the main limitation of this technique is the low adhesion of the anodized nanotubes arrays on titanium surface [92,149,150] that favors corrosion. However, this inconvenience appears when the anodizing electrolyte contains a high concentration of fluoride acid because it can attack the barrier oxide underlying the nanotubes layer. The adhesive strength of the nanotubes can be also increased by changing the anodizing mode. For example, a three-step procedure consisting of (i) potentiodynamic polarization from open circuit potential to the end potential, (ii) potentiostatic polarization at the end potential for a selected time, and (iii) potentiodynamic polarization to return to the open circuit potential has been proved to be successful [151]. A recent study [152] shows that the growth of a nanotubular oxide layer on Ti10Mo8Nb beta alloy by electrochemical anodization in an electrolyte composed of glycerol–water with low content of NH_4F allows a great adherence to the metal surface due to the electrochemical mechanism of passivation. In fact, the Ti10Mo8Nb alloy hydrolyzes in the electrolytic solution, forming a passive layer constituted by a mixed oxide ($TiO_2-Nb_2O_5-MoO_2$) at the metal–oxide interface and chemically dissolve at the oxide–solution interface.

Hernández-López et al. [106] investigated the corrosion resistance of porous oxides anodically grown on Ti13Nb13Zr alloy in PBS solution. Anodizing is performed in 1 M H_2SO_4 and 34.5 mM HF electrolyte. As expected, they found that nonanodized samples present higher corrosion rates in PBS solution than the anodized ones. Additionally, the passivity current density related to the nanoporous layer formation is strongly lower than that relating to the oxide grown on Ti13Nb13Zr by simple immersion in SBF [22]. They found a good correlation between the EIS results and interpretation in terms of

the nanostructure, thickness, corrosion resistance, and the SEM/TEM microstructural examination and electrochemical measurements.

The observations of Ti-13Zr-13Nb alloys preanodized at low HF concentration show a fine nanotubular structure with long nanotubes and different features depending on the phase (α and β). In phase β, nanotubes are smaller and shorter than in phase α, inducing possible localized corrosion phenomena [153–155]. Their corrosion resistance has been evaluated in the standard Ringer's solution by changing pH through HCl. The increase of corrosion resistance due to the anodic nanotubular oxide is connected to the high thickness of the film and the negligible infiltrations of the electrolyte into the nanocavities of the oxide structure well adherent to the alloy.

As discussed in Section 4, the PEO technique allows improving the surface bioactivity by the inclusion of Ca and P elements in the oxide layer. Kassem and Choe [156] studied the capability of PEO to produce good porous material for bioimplant applications using a β-Ti-Nb binary alloy at different Nb content. As reported in Figure 14, potentiodynamic polarization analysis in 0.9% NaCl shows the beneficial effect of PEO and Nb content on the corrosion parameters and passive film stability. The increase in Nb content affects the passivation behavior up to the formation of a double-layer oxide structure. The best performance is ascribed to the alloy β-Ti-30Nb that shows the lowest corrosion and passivation current density.

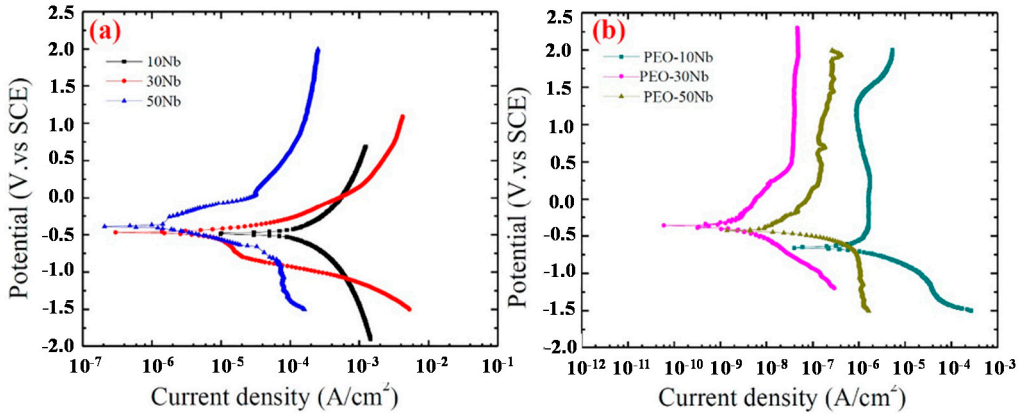

Figure 14. (**a**,**b**) Potentiodynamic polarization curves of the Ti-*x*Nb alloys before and after PEO treatment, respectively. Passive regions were observed in the case of the PEO-coated Ti-*x*Nb alloys. Reprinted from [156], copyright (2019), with permission from Elsevier.

Ti-20Nb-10Zr-5Ta alloys immersed in Hank's solution presented passivation with high potential levels up to 10 V; this behavior is attributed to the addition of Nb and Zr and generated O_2 evolution. In 0.9% wt.% NaCl, the alloy presents passivation with a reactive surface after 10 h of exposition. After 24 h, the surface is less reactive and presents lower corrosion current density because a more stable passive layer is formed after long times of immersion [71].

The characterization of Ti-Nb-Zr-Ta alloy coated by PEO and compared with Ti CP and Ti-6Al-4V alloys were studied by Cordeiro in 2018. EIS characterization related to surfaces treated by PEO in electrolytes of calcium acetate and glycerophosphate showed a diffusion system in SBF solution (Figure 11a); meanwhile, uncoated material surfaces showed only one time constant (Figure 11b). Ti-Nb-Zr-Ta and Ti-6Al-4V alloys present a similar behavior better than Ti CP [157]. Coated alloys have values of impedance modules of four orders higher than uncoated material. According to Cordeiro et al. and their discussion with other authors, high values at high frequencies indicate a dielectric property of porous or nanotubes structures, while an increase of frequency values in low frequencies range means a barrier effect [157–162]. When samples are in PP characterization, coatings present higher E_{corr} and lower i_{corr} than uncoated samples, meaning better corrosion resistance.

Ti-6Al-4V coated samples show an anodic breach instability on the metal surface, while Ti-Nb-Zr-Ta coated alloys exhibit a more stable behavior [157].

Finally, it is noteworthy that the possible combination of anodization process and PEO technique is a good strategy to assign excellent biocompatibility, bioactivity, and corrosion resistance to β-Ti alloys at the same time. Mazigi et al. [163] demonstrated that using this double procedure, Ti-35Nb-3Zr alloy acquires performance similar to conventional biomedical Ti-6Al-4V alloy (Figure 15). The biocompatibility experiments on Ti-35Nb-3Zr show similar results to Cp-Ti. In the bare condition, conventional Cp-Ti and Ti-6Al-4V have lower corrosion current density (of 30%); however, it can be observed that the passivation current density is lower for Ti-35Nb-3Zr alloy due to the benefits of niobium and zirconium to the oxide. After the combination of (i) electrochemical anodization to grow a nanoporous layer and (ii) calcium phosphate deposition by PEO, the corrosion performance of Ti-35Nb-3Zr alloy notable enhances at the level of Ti-6Al-4V alloy.

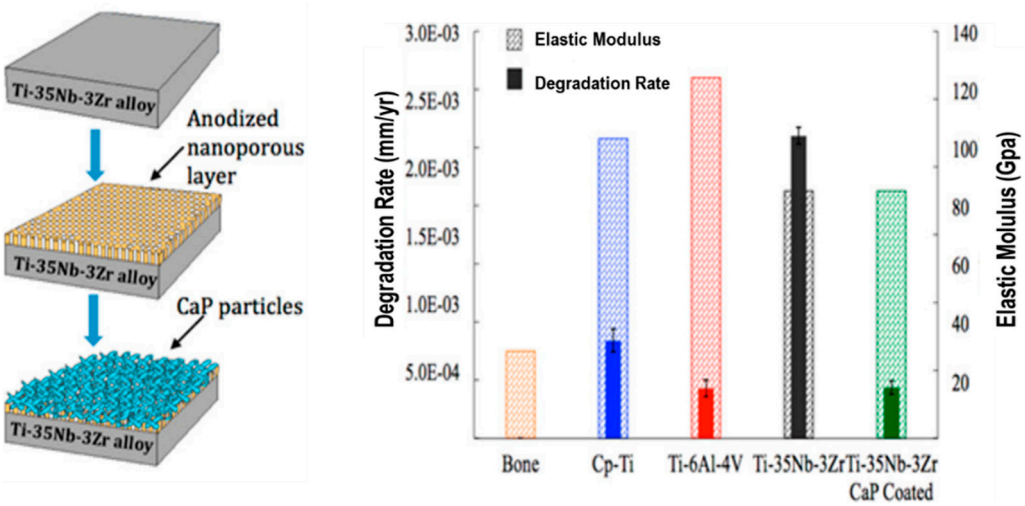

Figure 15. Comparing the degradation rate and elastic modulus of the conventional implant materials to the β-Ti-35Nb-3Zr alloy. Reprinted with permission from [163], copyright (2017) American Chemical Society.

Jaquez et al. [164,165] studied the behavior of titanium alloys (Cp-Ti, Ti-6Al-2Sn-4Zr-2Mo, and Ti-6Al-4V) in the presence of acid solutions and Hank's through potentiodynamic polarization and electrochemical noise. Statistical methods indicated that the passive layer created on Ti alloys surfaces is unstable; this condition is notable for Ti-6Al-2Sn-4Zr-2Mo in NaCl solution.

6. Outlook and Future Perspectives

This review reports and discusses the developments of Ti-6Al-4V and β-Ti alloys for biomedical applications by considering their microstructures, corrosion resistance, and passive layers. As they are used as biomedical implants, the essential interactions between the implants and human body environments are introduced. Due to the detrimental effect of Al and V, nontoxic β-Ti alloys are therefore developed. The primary alloying elements in most β-Ti alloys are Nb, Ta, and Zr, which are both β-stabilizer and biocompatible elements for the human body. According to the content of β-stabilizer, different microstructures, such as ω, β, and β′ phases, are found in different β-Ti alloys.

Afterward, the reason accounting for the good corrosion resistance of Ti and Ti alloys in body fluid is specified, which is attributed to the stable oxides formed on their surfaces. Therefore, the electrochemical corrosion of Ti alloys in a biological environment is significantly reviewed. Understanding if a Ti alloy with good corrosion resistance in the body environment is essential for the design of biomedical implants.

Although Ti and Ti alloys have significantly good corrosion resistance in the human body, fretting and wear are specifically involved. In these conditions, the spontaneously

formed passive state of titanium is not completely stable, and localized ruptures have been found on a microscopic scale. Consequently, strong degradation due to localized corrosion can occur on the surface of the material due to the reaction with corrosive agents. Therefore, surface modification is often carried out to improve the mechanical, biological, and chemical properties [166]. Therefore, passive and protective layers to be grown on the Ti and Ti alloys before implantation are required. Several surface modification methods, including electrochemical passivation, thermal oxidation, and plasma electrolytic oxidation, as well as the electrochemical characteristics of the produced layers (mainly consisted of TiO_2) on Ti-6Al-4V and β-Ti alloys, are introduced [97,167–172]. As summarized in Table 3, such-produced passive oxides generally have better corrosion resistance, compared to the naturally formed layers on the counterparts. Meanwhile, such-produced layers may contain some bioactive matter to increase the bioactivity of modified Ti alloys and thereby the affinity to bone cells.

According to the literature survey of this review, our vision is that the future of titanium alloys moves toward the use of β-phase alloys reinforced by anodic coatings. The analyzed research trend suggests that the exploitation of the electrochemical anodization technique, by searching the best conditions to optimize the performance of the oxide film in terms of corrosion stability and biocompatibility for a long time, could arrive at unprecedented goals. The electrochemical anodization technique offers versatility and precise control of the parameters of oxide growth, arriving, for example, at the perfect correlation of the anodizing potential to TiO_2 nanotubes size of the passive layer. Thus, intensive studies on the electrochemical processes in human body environments are expected in the next years. When necessary, the coupling of EA and PEO techniques can be adopted since a notable improvement of the coating performance is recorded in some cases. This is another chance that must be taken after the evaluation of costs and benefits. Another valuable approach that should be considered is the combination of experimental and predictive methods. In recent years, advances in machine learning and artificial intelligence immensely decoded and empowered allowed the modeling of the biomedical material interaction with surrounding tissue, providing biomedicine a modern tool to predict the biosafety and efficacy of a metallic implant. Thus, our view is that this theoretical approach could complement the need for the safety of biomedical alloys because potentially deciphers the quantitative nanostructure activity's relationship to corrosion metal leaching [173] and handles toxicity problems to the surrounding tissue during metal ion leaching from implants [174–176].

The importance of the topic, the growing interest in research, and the enormous unexplored potential of this literature review are intended to provide information on the methods of surface improvement by the formation of a corrosion-resistant passive oxide on biomedical Ti alloys in the human body fluids.

There are still some questions for β-Ti alloys used as implants. Further studies are still necessary to guarantee high durability in the human body and the research trend is to investigate β-Ti alloys with nontoxic elements, trying to improve corrosion resistance, mechanical properties, and biocompatibility to outstanding values. Therefore, lattice-structured β-Ti alloys with compatible elastic moduli coated by multifunctional materials, such as nanoceramics [177], may present an interesting future.

Table 3. Summary of the corrosion properties of passivated (spontaneous, in situ, or pre-formed oxide coating) Ti-6Al-4V and β-Ti alloys in different fluids.

Ti-Alloy	Passive Layer Formation (In Situ/Pre-Grown)	Biological Solution, T (°C), t_{IMM}* (h)	Corrosion Current Density/μA cm^{-2}	Corrosion Potential/V vs. Ag/AgCl	Main Conclusions in Terms of Corrosion Resistance	Ref.
Ti6Al4V	–	NaCl, 25	0.043	−0.538	Unstable passive layer.	[165]
Ti6Al4V	in situ, NTs	Hank's, 25, 168 Hank´s, 37, 168	0.104 0.164	−0.297 −0.304	At 25 °C: Ti and Ti6Al4V are similar. At 37 °C: corrosion resistance Ti–6Al–4V decreases due to passive film dissolution.	[117]
Ti6Al4V	in situ	PBS, 25, 0.33 PBS/BSA, 25, 0.33	0.18 0.75	−0.497 −0.495	Ti6Al4V alloy is better than Ti grade2 in PBS and PBS/BSA. In PBS/BSA, i_{corr} increases for Ti6Al4V and decreases for Ti Grade 2.	[127]
Ti35Nb2Ta3Zr	–	Hank´s, 37, 2	0.101	−0.320	The high corrosion resistance and satisfactory biocompatibility make the novel Ti35Nb3Zr2Ta alloy a promising biomaterial for surgical implants.	[159]
Cp-Ti	PEO	AS, 37, 0.16	5.6×10^{-5}	−0.0546	PEO surface treatment confers better electrochemical behavior to Ti alloys.	[160]
Cp-Ti	PEO 5 μm thick, porous oxide	AS at different pH (3.0, 6.5, and 9.0), SBF, 37, 0.16	PEO AS(0.00019) SBF (0.00014)	PEO AS(0.15) SBF (0.081)	PEO improves surface properties and electrochemical stability of Cp-Ti surface due to Anatase/Rutile formation, while increasing protein adsorption.	[161]
Ti6Al4V	PEO	SBF, 25, 336	0.488	−0.118	Long times of PEO increase pore size and facilitate the penetration of ions; the passivation range is reduced.	[123]
Ti6Al4V ELI	EA TiO_2 NTs	NaCl, 25	0.009	0.13	EA permits the growth of a thick oxide compact layer at the base of TiO_2 NTs array guaranteeing high corrosion resistance.	[131]
Ti-Nb-Zr-Ta	PEO	SBF, 37, 0.16	0.24	0.265	Electrochemical behavior similar to Ti6Al4V, but with less tendency to transport ions across the oxide film.	[157]
Ti-xNb	PEO	SBF, 37, 24	0.006	−0.353	PEO coating made on the Ti-30Nb alloy gives great corrosion resistance and good bioactivity	[156]
Ti6Al4V	EA TiO_2 NTs	NaCl, 25, 0.25	0.058	80.28	Ti6Al4V covered by TiO_2 NTs passive layer has higher corrosion resistance compared to the bare Ti6Al4V.	[132]

t_{IMM}* = immersion time.

Author Contributions: Conceptualization, P.B.; methodology, P.B.; data collection, P.B., P.L., F.A.-C.; J.D.C.T., and A.C.d.R.; formal analysis, P.B.; writing, P.B., P.L., F.A.-C., J.D.C.T., and A.C.d.R.; review and editing, P.B. and L.-Y.C.; supervision, P.B. and L.-Y.C. All authors have read and agreed to the published version of the manuscript.

Funding: Patrizia Bocchetta was funded by MIUR through the PRIN 2017 project support under the grant 2017948FEN (FASTire).

Institutional Review Board Statement: Not applicable.

Informed Consent Statement: Not applicable.

Acknowledgments: The authors acknowledge the Academic Body UANL—CA-316 "Deterioration and integrity of composite materials" and the student Jesus Manuel Jaquez.

Conflicts of Interest: The authors declare no conflict of interest.

References

1. Dini, C.; Costa, R.C.; Sukotjo, C.; Takoudis, C.G.; Mathew, M.T.; Barão, V.A.R. Progression of Bio-Tribocorrosion in Implant Dentistry. *Front. Mech. Eng.* **2020**, *6*, 1–14. [CrossRef]
2. Apaza-Bedoya, K.; Tarce, M.; Benfatti, C.A.M.; Henriques, B.; Mathew, M.T.; Teughels, W.; Souza, J.C.M. Synergistic interactions between corrosion and wear at titanium-based dental implant connections: A scoping review. *J. Periodontal Res.* **2017**, *52*, 946–954. [CrossRef] [PubMed]
3. Mehkri, S.; Abishek, N.R.; Sumanth, K.S.; Rekha, N. Study of the Tribocorrosion occurring at the implant and implant alloy Interface: Dental implant materials. *Mater. Today Proc.* **2020**. [CrossRef]
4. Cordeiro, J.M.; Barão, V.A.R. Is there scientific evidence favoring the substitution of commercially pure titanium with titanium alloys for the manufacture of dental implants? *Mater. Sci. Eng. C* **2017**, *71*, 1201–1215. [CrossRef]
5. Zhang, L.; Chen, L. A Review on Biomedical Titanium Alloys: Recent Progress and Prospect. *Adv. Eng. Mater.* **2019**, *21*, 1801215. [CrossRef]
6. Noronha Oliveira, M.; Schunemann, W.V.H.; Mathew, M.T.; Henriques, B.; Magini, R.S.; Teughels, W.; Souza, J.C.M. Can degradation products released from dental implants affect peri-implant tissues? *J. Periodontal Res.* **2017**, *6*, 1–11. [CrossRef] [PubMed]
7. Mombelli, A.; Hashim, D.; Cionca, N. What is the impact of titanium particles and biocorrosion on implant survival and complications? A critical review. *Clin. Oral Implant. Res.* **2018**, *29* (Suppl. 18), 37–53. [CrossRef] [PubMed]
8. Zhang, L.-C.; Chen, L.-Y.; Wang, L. Surface Modification of Titanium and Titanium Alloys: Technologies, Developments, and Future Interests. *Adv. Eng. Mater.* **2020**, *22*, 1901258. [CrossRef]
9. Dias Corpa Tardelli, J.; Bolfarini, C.; Cândido Dos Reis, A. Comparative analysis of corrosion resistance between beta titanium and Ti-6Al-4V alloys: A systematic review. *J. Trace Elem. Med. Biol.* **2020**, *62*, 126618. [CrossRef]
10. Dias Corpa Tardelli, J.; Lima da Costa Valente, M.; Theodoro de Oliveira, T.; Cândido dos Reis, A. Influence of chemical composition on cell viability on titanium surfaces: A systematic review. *J. Prosthet. Dent.* **2021**, *125*, 421–425. [CrossRef]
11. Sharma, A.; Oh, M.C.; Kim, J.T.; Srivastava, A.K.; Ahn, B. Investigation of electrochemical corrosion behavior of additive manufactured Ti–6Al–4V alloy for medical implants in different electrolytes. *J. Alloys Compd.* **2020**, *830*, 154620. [CrossRef]
12. Peñarrieta-Juanito, G.; Sordi, M.B.; Henriques, B.; Dotto, M.E.R.; Teughels, W.; Silva, F.S.; Magini, R.S.; Souza, J.C.M. Surface damage of dental implant systems and ions release after exposure to fluoride and hydrogen peroxide. *J. Periodontal Res.* **2018**, *54*, 46–52. [CrossRef] [PubMed]
13. Contu, F.; Elsener, B.; Böhni, H. A study of the potentials achieved during mechanical abrasion and the repassivation rate of titanium and Ti6Al4V in inorganic buffer solutions and bovine serum. *Electrochim. Acta* **2004**, *50*, 33–41. [CrossRef]
14. Mischler, S. Triboelectrochemical techniques and interpretation methods in tribocorrosion: A comparative evaluation. *Tribol. Int.* **2008**, *41*, 573–583. [CrossRef]
15. Ribeiro, A.R.; Gemini-Piperni, S.; Travassos, R.; Lemgruber, L.; Silva, R.C.; Rossi, A.L.; Farina, M.; Anselme, K.; Shokuhfar, T.; Shahbazian-Yassar, R. Trojan-Like Internalization of Anatase Titanium Dioxide Nanoparticles by Human Osteoblast. *Cells Sci. Rep.* **2016**, *6*, 23615. [CrossRef]
16. Mano, S.S.; Kanehira, K.; Taniguchi, A. Comparison of cellular uptake and inflammatory response via toll-like receptor 4 to lipopolysaccharide and titanium dioxide nanoparticles. *Int. J. Mol. Sci.* **2013**, *14*, 13154–13170. [CrossRef]
17. Okuda-Shimazaki, J.; Takaku, S.; Kanehira, K.; Sonezaki, S.; Taniguchi, A. Effects of titanium dioxide nanoparticle aggregate size on gene expression. *Int. J. Mol. Sci.* **2010**, *11*, 2383–2392. [CrossRef]
18. Chen, L.-Y.; Cui, Y.-W.; Zhang, L.-C. Recent Development in Beta Titanium Alloys for Biomedical Applications. *Metals* **2020**, *10*, 1139. [CrossRef]
19. Kolawole, S.K.; Hai, W.; Zhang, S.; Sun, Z.; Siddiqui, M.A.; Ullah, I.; Song, W.; Witte, F.; Yang, K. Preliminary study of microstructure, mechanical properties and corrosion resistance of antibacterial Ti-15Zr-xCu alloy for dental application. *J. Mater. Sci. Technol.* **2020**, *50*, 31–43. [CrossRef]

20. Kazemi, M.; Ahangarani, S.; Esmailian, M.; Shanaghi, A. Investigation on the corrosion behavior and biocompatibility of Ti-6Al-4V implant coated with HA/TiN dual layer for medical applications. *Surf. Coat. Technol.* **2020**, *397*, 126044. [CrossRef]
21. Guo, W.Y.; Sun, J.; Wu, J.S. Electrochemical and XPS studies of corrosion behavior of Ti–23Nb–0.7Ta–2Zr–O alloy in Ringer's solution. *Mater. Chem. Phys.* **2009**, *113*, 816–820. [CrossRef]
22. Shukla, K.A.; Balasubramaniam, R. Effect of surface treatment on electrochemical behavior of CP Ti, Ti–6Al–4V and Ti–13Nb–13Zr alloys in simulated human body fluid. *Corros. Sci.* **2006**, *48*, 1696–1720. [CrossRef]
23. Zhou, Y.L.; Niinomi, M.; Akahori, T.; Fukui, H.; Toda, H. Corrosion resistance and biocompatibility of Ti–Ta alloys for biomedical applications. *Mater. Sci. Eng. A* **2005**, *398*, 28–36. [CrossRef]
24. Oliveira, T.T.; Reis, A.C. Fabrication of dental implants by the additive manufacturing method: A systematic review. *J. Prosthet. Dent.* **2019**, *122*, 270–274. [CrossRef]
25. Kaseem, M.; Choe, H.C. Simultaneous improvement of corrosion resistance and bioactivity of a titanium alloy via wet and dry plasma treatments. *J. Alloys Compd.* **2021**, *851*, 156840. [CrossRef]
26. Xie, L.; Liu, C.; Song, Y.; Guo, H.; Wang, Z.; Hua, L.; Wang, L.; Zhang, L.C. Evaluation of microstructure variation of TC11 alloy after electroshocking treatment. *J. Mater. Res. Technol.* **2020**, *9*, 2455–2466. [CrossRef]
27. Pérez, D.A.G.; Jorge Junior, A.M.; Roche, V.; Lepretre, J.C.; Afonso, C.R.M.; Travessa, D.N.; Asato, G.H.; Bolfarini, C.; Botta, W.J. Severe plastic deformation and different surface treatments on the biocompatible Ti13Nb13Zr and Ti35Nb7Zr5Ta alloys: Microstructural and phase evolutions, mechanical properties, and bioactivity analysis. *J. Alloys Compd.* **2020**, *812*. [CrossRef]
28. Konovalov, S.; Komissarova, I.; Ivanov, Y.; Gromov, V.; Kosinov, D. Structural and phase changes under electropulse treatment of fatigue-loaded titanium alloy VT1-0. *J. Mater. Res. Technol.* **2019**, *8*, 1300–1307. [CrossRef]
29. Brammer, K.S.; Oh, S.; Cobb, C.J.; Bjursten, L.M.; van der Heyde, H. Improved bone-forming functionality on diameter-controlled TiO_2 nanotube surface. *Acta Biomater.* **2009**, *5*, 3215–3223. [CrossRef]
30. Antunes, A.R.; De Oliveira, L.C.M. Corrosion fatigue of biomedical metallic alloys: Mechanisms and mitigation. *Acta Biomater.* **2012**, *8*, 937–962. [CrossRef]
31. Yazdi, R.; Ghasemi, M.H.; Wang, C.; Neville, A. Bio-corrosion behaviour of oxygen diffusion layer on Ti-6Al-4V during tribocorrosion. *Corros. Sci.* **2017**, *128*, 23–32. [CrossRef]
32. Lutjering, G.; Williams, C.J. *Titanium*, 2nd ed.; Springer: Berlin/Heidelberg, Germany, 2007.
33. Attanasio, A.; Gelfi, M.; Pola, A.; Ceretti, E.; Giardini, C. Influence of Material Microstructures in Micromilling of Ti6Al4V Alloy. *Materials* **2013**, *6*, 4268–4283. [CrossRef] [PubMed]
34. Geetha, M.; Singh, K.A.; Asokamani, R.; Gogia, K.A. Ti based biomaterials, the ultimate choice for orthopaedic implants—A review. *Prog. Mater. Sci.* **2009**, *54*, 397–425. [CrossRef]
35. Sidambe, T.A. Biocompatibility of Advanced Manufactured Titanium Implants—A Review. *Materials* **2014**, *7*, 8168–8188. [CrossRef]
36. Cvijović-Alagić, I.; Cvijović, Z.; Mitrović, S.; Panić, V.; Rakin, M. Wear and corrosion behaviour of Ti–13Nb–13Zr and Ti–6Al–4V alloys in simulated physiological solution. *Corros. Sci.* **2011**, *53*, 796–808. [CrossRef]
37. Atapour, M.; Pilchak, A.; Frankel, S.G.; Williams, C.J.; Fathi, H.M.; Shamanian, M. Corrosion Behavior of Ti-6Al-4V with Different Thermomechanical Treatments and Microstructures. *Corrosion* **2010**, *66*, 065004. [CrossRef]
38. Cvijović-Alagić, I.; Cvijović, Z.; Bajat, J.; Rakin, M. Composition and processing effects on the electrochemical characteristics of biomedical titanium alloys. *Corrs. Sci.* **2014**, *83*, 245–254. [CrossRef]
39. Luiz de Assis, S.; Wolynec, S.; Costa, I. Corrosion characterization of titanium alloys by electrochemical techniques. *Electrochim. Acta* **2006**, *51*, 1815–1819. [CrossRef]
40. Milošev, I.; Metikoš-Hukovic´, M.; Strehblow, H.H. Passive film on orthopaedic TiAlV alloy formed in physiological solution investigated by X-ray photoelectron spectroscopy. *Biomaterials* **2000**, *21*, 2103–2113. [CrossRef]
41. Metikoš-Hukovic, M.; Kwokal, A.; Piljac, J. The influence of niobium and vanadium on passivity of titanium-based implants in physiological solution. *Biomaterials* **2003**, *24*, 3765–3775. [CrossRef]
42. Marino, C.E.; Biaggio, S.R.; Rocha-Filho, R.C.; Bocchi, N. Voltammetric stability of anodic films on the Ti6Al4V alloy in chloride medium. *Electrochim. Acta* **2006**, *51*, 6580–6583.
43. Mirza, A.; King, A.; Troakes, C.; Exley, C. Aluminium in brain tissue in familial Alzheimer's disease. *J. Trace Elem. Med. Biol.* **2017**, *40*, 30–36. [CrossRef] [PubMed]
44. Moretti, B.; Pesce, V.; MacCagnano, G.; Vicenti, G.; Lovreglio, P.; Soleo, L.; Apostoli, P. Peripheral neuropathy after hip replacement failure: Is vanadium the culprit? *Lancet* **2012**, *379*. [CrossRef]
45. Akahori, T.; Niinomi, M.; Fukui, H.; Suzuki, A.; Hattori, Y.; Niwa, S. *Ti-2003, Science and Technology*; Wiley-VCH: Weinheim, Germany, 2004; p. 3181.
46. Qazi, J.I.; Tsakiris, V.; Marquard, B.; Rack, H.J. *Ti-2003, Science and Technology*; WileyVCH: Weinheim, Germany, 2004; p. 1651.
47. Qazi, J.; Rack, H. Metastable Beta Titanium Alloys for Orthopedic Applications. *Adv. Eng. Mater.* **2005**, *7*, 993–998. [CrossRef]
48. Atapour, M.; Pilchak, L.A.; Frankel, S.G.; Williams, C.J. Corrosion behavior of β titanium alloys for biomedical applications. *Mater. Sci. Eng. C* **2011**, *31*, 885–891. [CrossRef]
49. Pourbaix, M. *Atlas of Electrochemical Equilibria in Aqueous Solution*, 2nd ed.; National Association of Corrosion Engineers: Houston, TX, USA, 1974; p. 219.
50. Kurup, A.; Dhatrak, P.; Khasnis, N. Surface modification techniques of titanium and titanium alloys for biomedical dental applications: A review. *Mater. Today Proc.* **2021**, *39*, 84–90. [CrossRef]

51. Chen, P.C.; Hsieh, S.J.; Chen, C.C.; Zou, J. The Microstructure and Capacitance Characterizations of Anodic Titanium Based Alloy Oxide Nanotube. *J. Nanomater.* **2013**, *2013*, 1–9. [CrossRef]
52. Pedeferri, P. *Corrosion Science and Engineering*; Lazzari, L., Pedeferri, M.P., Eds.; Springer Nature Switzerland AG: Cham, Switzerland, 2018.
53. Hussein, M.A.; Kumar, M.; Drew, R.; Al-Aqeeli, N. Electrochemical Corrosion and In Vitro Bioactivity of Nano-Grained Biomedical Ti-20Nb-13Zr Alloy in a Simulated Body Fluid. *Materials* **2018**, *11*, 26. [CrossRef]
54. FKing, F.; Shoesmith, D. 13—Nuclear waste canister materials, corrosion behaviour and long-term performance in geological repository systems. In *Woodhead Publishing Series in Energy, Geological Repository Systems for Safe Disposal of Spent Nuclear Fuels and Radioactive Waste*; Ahn, J., Michael, J.A., Eds.; Woodhead Publishing: Cambridge, UK, 2010; pp. 379–420. [CrossRef]
55. Tschernitschek, H.; Borchers, L.; Geurtsen, W. Nonalloyed titanium as a bioinert metal–A review. *Quintessence Int.* **2005**, *36*, 523–530. [CrossRef]
56. Jacobs, J.J.; Gilbert, J.L.; Urban, R.M. Corrosion of metal orthopaedic implants. *J. Bone Jt. Surg.* **1998**, *80-A*, 268. [CrossRef]
57. Gilbert, J.L.; Buckley, C.A.; Jacobs, J.J. In vivo corrosion of modular hip prothesis components in mixed and similar metal combinations. The effect of crevice, stress, motion, and alloy coupling. *J. Biomed. Mater. Res.* **1993**, *27*, 1533. [CrossRef]
58. Grosgogeat, B.; Reclaru, L.; Lissac, M.; Dalard, F. Measurement and evaluation of galvanic corrosion between titanium/Ti6Al4V implants and dental alloys by electrochemical techniques and auger spectrometry. *Biomaterials* **1999**, *20*, 933. [CrossRef]
59. Noumbissi, S.; Scarano, A.; Gupta, S. A Literature Review Study on Atomic Ions Dissolution of Titanium and Its Alloys in Implant Dentistry. *Materials* **2019**, *12*, 368. [CrossRef]
60. Virtanen, S. Corrosion of biomedical implant materials. *Corros. Rev.* **2008**, *26*, 147–171. [CrossRef]
61. Manivasagam, G.; Dhinasekaran, D.; Rajamanickam, A. Biomedical implants: Corrosion and its prevention—A review. *Recent Patents Corros. Sci.* **2010**, *2*, 40–54. [CrossRef]
62. Gilbert, J.L.; Mali, S. Medical implant corrosion: Electrochemistry at metallic biomaterial surfaces. In *Degradation of Implant Materials*; Chapter 1; Eliaz, N., Ed.; Springer: New York, NY, USA, 2012; pp. 1–28.
63. Virtanen, S. Degradation of titanium and its alloys. In *Degradation of Implant Materials*; Chapter 2; Eliaz, N., Ed.; Springer: New York, NY, USA, 2012; pp. 29–55.
64. Witte, F.; Eliezer, A. Biodegradable metals. In *Degradation of Implant Materials*; Chapter 5; Eliaz, N., Ed.; Springer: New York, NY, USA, 2012; pp. 93–109.
65. Pound, B.G. Corrosion behavior of metallic materials in biomedical applications. I. Ti and its alloys. *Corros. Rev.* **2014**, *32*, 1–20. [CrossRef]
66. Eliaz, N. Corrosion of Metallic Biomaterials: A Review. *Materials* **2019**, *12*, 407. [CrossRef] [PubMed]
67. Han, Y.; Xu, K. Photoexcited formation of bone apatite-like coatings on micro-arc oxidazed titanium. *J. Biomed. Mater. Res.* **2004**, *71A*, 608–614. [CrossRef]
68. Landolt, D. (Ed.) *Corrosion and Surface Science*; CRC Press Taylor and Francis Group: Boca Raton, FL, USA, 2007; p. 33487.
69. Lohrengel, M.M. Formation of ionic space charge layers in oxide films on valve metals. *Electrochim. Acta* **1994**, *39*, 1265–1271. [CrossRef]
70. Tinghua, L.; Chongjian, D.; Yupeng, L.; Jun, W.; Xia, Z.; Xiaowei, G.; Wei, Z.; Daoai, W.; Donglai, Z. An Anodized Titanium/Sol-Gel Composite Coating with Self-Healable Superhydrophobic and Oleophobic Property. *Front. Mater.* **2021**, *8*, 64. [CrossRef]
71. Milosev, I.; Popa, M. Electrochemical properties, chemical composition and thickness of passive film formed on novel Ti–20Nb–10Zr–5Ta alloy. *Electrochim. Acta* **2013**, *99*, 176–189. [CrossRef]
72. Jarosz, M.; Grudzień, J.; Kapusta-Kołodziej, J.; Chudecka, A.; Sołtys, M.; Sulka, G.D. Chapter seven-Anodization of titanium alloys for biomedical applications. In *Micro and Nano Technologies, Nanostructured Anodic Metal Oxides*; Sulka, G.D., Ed.; Elsevier: Krakow, Poland, 2020; Volume 7, pp. 211–275.
73. Zwilling, V.; Aucouturier, M.; Darque-Ceretti, E. Anodic oxidation of titanium and TA6V alloy in chromic media. An electrochemical approach. *Electrochim. Acta* **1999**, *45*, 921–929. [CrossRef]
74. Cheng, Y.; Yang, H.; Yang, Y.; Huang, J.; Wu, K.; Chen, Z.; Wang, X.; Lin, C.; Lai, Y. Progress in TiO_2 nanotube coatings for biomedical applications: A review. *J. Mater. Chem. B* **2018**, *6*, 1862–1886. [CrossRef] [PubMed]
75. Lin, N.; Li, D.; Zou, J.; Xie, R.; Wang, Z.; Tang, B. Surface Texture-Based Surface Treatments on Ti6Al4V Titanium Alloys for Tribological and Biological Applications: A Mini Review. *Materials* **2018**, *11*, 487. [CrossRef] [PubMed]
76. Michalska-Domańska, M.; Łazińska, M.; Łukasiewicz, J.; Mol, J.M.C.; Durejko, T. Self-Organized Anodic Oxides on Titanium Alloys Prepared from Glycol- and Glycerol-Based Electrolytes. *Materials* **2020**, *13*, 4743. [CrossRef]
77. Gulati, K.; Sinn Aw, M.; Findlay, D.; Losic, D. Local drug delivery to the bone by drug-releasing implants: Perspectives of nano-engineered titania nanotube arrays. *Ther. Deliv.* **2012**, *3*, 857–873. [CrossRef]
78. Luz, A.R.; Santos, L.S.; Lepienski, C.M.; Kuroda, P.B.; Kuromoto, N.K. Characterization of the morphology, structure and wettability of phase dependent lamellar and nanotube oxides on anodized Ti-10Nb alloy. *Appl. Surf. Sci.* **2018**, *448*, 30–40. [CrossRef]
79. Dikicia, T.; Erola, M.; Toparlia, M.; Celika, E. Characterization and photocatalytic properties of nanoporous titanium dioxide layer fabricated on pure titanium substrates by the anodic oxidation process. *Ceram. Int.* **2014**, *40*, 1587–1591. [CrossRef]
80. Gao, A.; Hang, R.; Bai, L.; Tang, B.; Chu, P.K. Electrochemical surface engineering of titanium-based alloys for biomedical application. *Electrochim. Acta* **2018**, *271*, 699–718. [CrossRef]

81. Indira, K.; Kamachi Mudali, U.; Nishimura, T.; Rajendran, N. A Review on TiO_2 Nanotubes: Influence of Anodization Parameters, Formation Mechanism, Properties, Corrosion Behavior, and Biomedical Applications. *J. Biol. Tribo-Corros.* **2015**, *1*, 28. [CrossRef]
82. Macak, M.J.; Tsuchiya, H.; Ghicov, A.; Yasuda, K.; Hahn, R.; Bauer, S.; Schmuki, P. TiO_2 nanotubes: Self-organized electrochemical formation, properties and applications. *Curr. Opin. Solid State Mater. Sci.* **2007**, *11*, 3–18. [CrossRef]
83. Poddar, S.; Bit, A.; Sinha, S.K. A study on influence of anodization on the morphology of titania nanotubes over Ti6Al4V alloy in correlation to hard tissue engineering application. *Mater. Chem. Phys.* **2020**, *254*, 123457. [CrossRef]
84. Sarraf, M.; Nasiri-Tabrizi, B.; Yeong, C.H.; Madaah Hosseini, H.R.; Saber-Samandari, S.; Basirun, W.J.; Tsuzuki, T. Mixed oxide nanotubes in nanomedicine: A dead-end or a bridge to the future? *Ceram. Int.* **2021**, *47*, 2917–2948. [CrossRef]
85. Rajyalakshmi, A.; Ercan, B.; Balasubramanian, K.; Webster, T.J. Reduced adhesion of macrophages on anodized titanium with select nanotube surface features. *Int. J. Nanomed.* **2011**, *6*, 1765–1771. [CrossRef]
86. Tsuchiya, H.; Macak, J.M.; Muller, L.; Kunze, J.; Muller, F. Hydroxyapatite growth on anodic TiO_2 nanotubes. *J. Biol. Mater. Res. Part A* **2006**, *77A*, 534–541. [CrossRef]
87. von Wilmowsky, C.; Bauer, S.; Roedl, S.; Neukam, F.W.; Schmuki, P. The diameter of anodic TiO_2 nanotubes affects bone formation and correlates with the bone morphogenetic protein-2 expression in vivo. *Clin. Oral. Implant. Res.* **2012**, *23*, 359–366. [CrossRef] [PubMed]
88. Simchi, A.; Tamjid, E.; Pishbin, F.; Boccaccini, A.R. Recent progress in inorganic and composite coatings with bactericidal capability for orthopaedic applications. *Nanomed. Nano Biol. Med.* **2011**, *7*, 22–39. [CrossRef]
89. Swain, S.; Misra, R.D.K.; You, C.K.; Rautray, T.R. TiO_2 nanotubes synthesised on Ti-6Al-4V ELI exhibits enhanced osteogenic activity: A potential next-generation material to be used as medical implants. *Mater. Technol.* **2020**. [CrossRef]
90. Minagar, S.; Berndt, C.C.; Wang, J.; Ivanova, E.; Wen, C. A review of the application of anodization for the fabrication of nanotubes on metal implant surfaces. *Acta Biol.* **2012**, *8*, 2875–2888. [CrossRef]
91. Tsuchiya, H.; Akaki, T.; Nakata, J.; Terada, D.; Tsuji, N.; Koizumi, Y.; Minamino, Y.; Schmuki, P.; Fujimoto, S. Anodic oxide nanotube layers on Ti–Ta alloys: Substrate composition, microstructure and self-organization on two-size scales. *Corros. Sci.* **2009**, *51*, 1528–1533. [CrossRef]
92. Martínez, C.; Guerra, C.; Silva, D.; Cubillos, M.; Briones, F.; Muñoz, L.; Páez, M.A.; Aguilar, C.; Sancy, M. Effect of porosity on mechanical and electrochemical properties of Ti-6Al-4V alloy. *Electrochim. Acta* **2020**, *338*, 135858. [CrossRef]
93. Assis, S.L.; Wolynec, S.; Costa, I. The electrochemical behaviour of Ti–13Nb–13Zr alloy in various solutions. *Mater. Corros.* **2008**, *59*, 739–743. [CrossRef]
94. Popa, M.V.; Raducanu, V.; Vasilescu, E.; Drob, P.; Cojocaru, D.; Vasilescu, C.; Ivanescu, S.; Mirza Rosca, J.C. Mechanical and corrosion behaviour of a Ti–Al–Nb alloy after deformation at elevated temperatures. *Mater. Corros.* **2008**, *59*, 919–928. [CrossRef]
95. Li, L.; Yu, K.; Zhang, K.; Liu, Y. Study of Ti–6Al–4V alloy spectral emissivity characteristics during thermal oxidation process. *Int. J. Heat Mass Transf.* **2016**, *101*, 699–706. [CrossRef]
96. Jamesh, M.; Sankara Narayanan, T.S.N.; Chu, P.K. Thermal oxidation of titanium: Evaluation of corrosion resistance as a function of cooling rate. *Mater. Chem. Phys.* **2013**, *138*, 565–572. [CrossRef]
97. Liu, X.; Chu, P.K.; Ding, C. Surface modification of titanium, titanium alloys, and related materials for biomedical applications. *Mater. Sci. Eng. R Rep.* **2004**, *47*, 49–121. [CrossRef]
98. Ma, K.; Zhang, R.; Sun, J.; Liu, C. Oxidation Mechanism of Biomedical Titanium Alloy Surface and Experiment. *Int. J. Corros.* **2020**, 1678615. [CrossRef]
99. Zheng, L.; Qian, S.; Liu, X. Enhanced osteogenic activity and bacteriostatic effect of TiO_2 coatings via hydrogen ion implantation. *Mater. Lett.* **2019**, *253*, 95–98. [CrossRef]
100. Li, L.; Kong, Y.; Kim, H.; Kim, Y.; Kim, H.; Heo, S.; Koak, J. Improved biological performance of Ti implants due to surface modification by micro-arc oxidation. *Biomaterials* **2004**, *25*, 2867–2875. [CrossRef]
101. Song, W.H.; Jun, Y.K.; Han, Y.; Hong, S.H. Biomimetic apatite coatings on micro-arc oxidized titania. *Biomaterials* **2004**, *25*, 3341. [CrossRef]
102. Fadl-allah, S.A.; Mohsen, Q. Characterization of native and anodic oxide films formed on commercial pure titanium using electrochemical properties and morphology techniques. *Appl. Surf. Sci.* **2010**, *256*, 5849–5855. [CrossRef]
103. Bundy, J.K. Corrosion and other electrochemical aspects of biomaterials. *Crit. Rev. Biomed. Eng.* **1993**, *22*, 139–251.
104. Rogers, S.D.; Howie, D.W.; Graves, S.E.; Pearcy, M.J.; Haynes, D.R. In vitro human monocyte response to wear particles of titanium alloy containing vanadium or niobium. *J. Bone Jt. Surg.* **1997**, *79*, 311–315. [CrossRef]
105. Bigi, A.; Nicoli-Aldini, N.; Bracci, B.; Zavan, B.; Boanini, E.; Sbaiz, F.; Panzavolta, S.; Zorzato, G.; Giardino, R.; Facchini, A.; et al. In vitro culture of mesenchymalcellsontonanocrystallinehydroxyapatite-coated Ti13Nb13Zr alloy. *J. Biomed. Mater. Res. Part A* **2007**, 213–221. [CrossRef] [PubMed]
106. Hernández-López, J.M.; Conde, A.; De Damborenea, J.; Arenas, M.A. Correlation of the nanostructure of the anodic layers fabricated on Ti-13Nb-13Zr with the electrochemical impedance response. *Corros. Sci.* **2015**, *94*, 61–69. [CrossRef]
107. Hao, Y.Q.; Li, S.J.; Hao, Y.L.; Zhao, Y.L.; Ai, H.J. Effect of nanotube diameters on bioactivity of multifunctional titanium alloy. *Appl. Surf. Sci.* **2013**, *268*, 44–51. [CrossRef]
108. Mendonça, G.; Mendonça, D.B.; Simões, L.G.; Araújo, A.L.; Leite, E.R.; Duarte, W.R.; Aragão, F.; Cooper, L. The effects of implant surface nanoscale features on osteoblast specific gene expression. *Biomaterials* **2009**, *30*, 4053–4062. [CrossRef]

109. Yamazoe, M. Study of corrosion of combinations of titanium/Ti-6Al-4V implants and dental alloys. *Dent. Mater. J.* **2010**, *29*, 542–553. [CrossRef] [PubMed]
110. Chen, X.; Shah, K.; Dong, S.; Peterson, L.; Callagon La Plante, E.; Sant, G. Elucidating the corrosion-related degradation mechanisms of a Ti-6Al-4V dental implant. *Natl. Library Med.* **2020**, *36*, 431–441. [CrossRef]
111. Wheelis, S.E.; Gindri, I.M.; Valderrama, P.; Wilson, T.G.; Huang, J.; Rodrigues, D.C. Effects of decontamination solutions on the surface of titanium: Investigation of surface morphology, composition, and roughness. *Clin. Oral Implant. Res.* **2016**, *27*, 329–340. [CrossRef]
112. Souza, J.C.; Barbosa, S.L.; Ariza, E.A.; Henriques, M.; Teughels, W.; Ponthiaux, P.; Rocha, L.A. How do titanium and Ti6Al4V corrode in fluoridated medium as found in the oral cavity? An in vitro study. *Mater. Sci. Eng. C* **2015**, *47*, 384–393. [CrossRef]
113. Nakagawa, M.; Matsuya, S.; Udoh, K. Effects of fluoride and dissolved oxygen concentrations on the corrosion behavior of pure titanium and titanium alloys. *Dent. Mater. J.* **2002**, *21*, 83–92. [CrossRef]
114. Faverani, L.P.; Barao, V.A.; Ramalho-Ferreira, G.; Ferreira, M.B.; Garcia-Junior, I.R.; Assuncao, W.G. Effect of bleaching agents and soft drink on titanium surface topography. *J. Biomed. Mater. Res. Part B Appl. Biomater.* **2013**, *102*, 22–30. [CrossRef]
115. Yu, F.; Addison, O.; Davenport, A.J. A synergistic effect of albumin and H_2O_2 accelerates corrosion of Ti6Al4V. *Acta Biomater.* **2015**, *26*, 355–365. [CrossRef]
116. Romesburg, J.W.; Wasserman, P.L.; Schoppe, C.H. Metallosis and metal- induced synovitis following total knee arthroplasty: Review of radiographic and CT findings. *J. Radiol. Case Rep.* **2010**, *4*, 7–17. [CrossRef]
117. Alves, V.A.; Reis, R.Q.; Santos, I.C.B.; Souza, D.G.; Gonçalves, T.D.F.; Pereira-Da-Silva, M.A.; Rossi, A.; Silva, L.A.D. In Situ impedance spectroscopy study of the electrochemical corrosion of Ti and Ti–6Al–4V in simulated body fluid at 25 °C and 37 °C. *Corros. Sci.* **2009**, *51*, 2473–2482. [CrossRef]
118. Costa, B.C.; Tokuhara, C.K.; Rocha, L.A.; Oliveira, R.C.; Lisboa-Filho, P.N.; Pessoa, J.C. Vanadium ionic species from degradation of Ti-6Al-4V metallic implants: In vitro cytotoxicity and speciation evaluation. *Mater. Sci. Eng. C* **2019**, *96*, 730–739. [CrossRef]
119. Pan, J.; Thierry, D.; Leygraf, C. Electrochemical and XPS studies of titanium for biomaterial application with respect to the effect of hydrogen peroxide. *J. Biomed. Mater. Res.* **1994**, *28*, 113–122. [CrossRef]
120. Galstyan, V.; Vomiero, A.; Comini, E.; Faglia, G.; Sberveglieri, G. TiO_2 nanotubular and nanoporous arrays by electrochemical anodization on different substrates. *RSC Adv.* **2011**, *1*, 1038–1044. [CrossRef]
121. Ibriş, N.; Mirza Rosca, J.C. EIS study of Ti and its alloys in biological media. *J. Electroanal. Chem.* **2002**, *526*, 53–62. [CrossRef]
122. Tamilselvi, S.; Raman, V.; Rajendran, N. Corrosion behaviour of Ti-6Al-7Nb and Ti-6Al-4V ELI alloys in the simulated body fluid solution by electrochemical impedance spectroscopy. *Electrochim. Acta* **2006**, *52*, 839–846. [CrossRef]
123. Nabavi, F.H.; Aliofkhazraei, M. Morphology, composition and electrochemical properties of bioactive-TiO_2/HA on CP-Ti and Ti6Al4V substrates fabricated by alkali treatment of hybrid plasma electrolytic oxidation process (estimation of porosity from EIS. *Surf. Coat. Technol.* **2019**, *375*, 266–291. [CrossRef]
124. Orazem, E.N.; Tribollet, B. *Electrochemical Impedance Spectroscopy*; John Wiley & Sons, Inc.: Hoboken, NJ, USA, 2017.
125. Attabi, S.; Mokhtari, M.; Taibi, Y.; Abdel-Rahman, I.; Hafez, B.; Elmsellem, H. Electrochemical and Tribological behavior of surface-treated titanium alloy Ti-6Al-4V. *J. Bio- Tribo-Corros.* **2019**, *5*, 2. [CrossRef]
126. Fraoucene, H.; Sugiawati, V.A.; Hatem, D.; Vacandio, F.; Eyraud, M.; Pasquinelli, M.; Djenizian, T. Optical and Electrochemical Properties of Self-Organized TiO_2 Nanotube Arrays From Anodized Ti-6Al-4V Alloy. *Front. Chem.* **2019**, *7*, 66. [CrossRef]
127. Dimah, K.M.; Albeza, F.; Borrás, A.V.; Muñoz, I. Study of the biotribocorrosion behaviour of titanium biomedical alloys in simulated body fluids by electrochemical techniques. *Wear* **2012**, *294*, 409–418. [CrossRef]
128. Durdu, S.; Usta, M.; Berkem, S.A. Bioactive coatings on Ti6Al4V alloy formed by plasma electrolytic oxidation. *Surf. Coat. Technol.* **2016**, *301*, 85–93. [CrossRef]
129. Souza, M.E.P.; Ballester, M.; Freire, C.M.A. EIS characterisation of Ti anodic oxide porous films formed using modulated potential. *Surf. Coat. Technol.* **2007**, *201*, 7775–7780. [CrossRef]
130. Nabavi, H.F.; Aliofkhazraei, M.; Rouhaghdam, A.S. Electrical characteristics and discharge properties of hybrid plasma electrolytic oxidation on titanium. *J. Alloys Compd.* **2017**, *728*, 464–475. [CrossRef]
131. Lario, J.; Viera, M.; Vicente, A.; Igual, A.; Amigó, V. Corrosion behaviour of Ti-6Al-4V ELI nanotubes for biomedical applications. *J. Mater. Sci. Technol.* **2019**, *8*, 5548–5556. [CrossRef]
132. Saha, S.K.; Park, Y.J.; Cho, S.O. Fabrication of highly ordered nanoporous oxide layer on Ti6Al4V surfaces for improved corrosion resistance property. *J. Mol. Struct.* **2021**, *1223*, 129244. [CrossRef]
133. Hussein, A.H.; Gepreel, M.A.H.; Gouda, M.K.; Hefnawy, A.M.; Kandil, S.H. Biocompatibility of new Ti–Nb–Ta base alloys. *Mater. Sci. Eng. C* **2016**, *61*, 574–578. [CrossRef] [PubMed]
134. Milosev, I.; Kosec, T.; Strehblow, H.-H. XPS and EIS study of the passive film formed on orthopaedic Ti–6Al–7Nb alloy in Hank's physiological solution. *Electrochim. Acta* **2008**, *53*, 3547–3558. [CrossRef]
135. Wei, T.; Huang, J.; Chao, C.Y.; Wei, L.; Tsai, M.; Chen, Y. Microstructure and elastic modulus evolution of TiTaNb alloys. *J. Mech. Behav. Biomed. Mater.* **2018**, *86*, 224–231. [CrossRef] [PubMed]
136. Chen, Y.H.; Chuang, W.S.; Huang, J.C.; Wang, X.; Chou, H.S.; Lai, Y.J.; Lin, P.H. On the bio-corrosion and biocompatibility of TiTaNb medium entropy alloy films. *Appl. Surf. Sci.* **2020**, *508*, 145307. [CrossRef]
137. Kim, S.; Choe, H. Highly ordered nanotube formation on beta typed Ti–xTa alloy surface. *J. Nanosci. Nanotechnol.* **2020**, *20*, 5791–5795. [CrossRef] [PubMed]

138. Choe, H.-C. Nanotubular surface and morphology of Ti-binary and Ti-ternary alloys for biocompatibility. *Thin Solid Films* **2011**, *519*, 4652–4657. [CrossRef]
139. Feng, X.; Macak, J.M.; Schmuki, P. Flexible self-organization of two size-scales oxide nanotubes on Ti45Nb alloy. *Electrochem. Commun.* **2007**, *9*, 2403–2407. [CrossRef]
140. Jang, S.-H.; Choe, H.-C.; Ko, Y.-M.; Brantley, W.A. Electrochemical characteristics of nanotubes formed on Ti–Nb alloys. *Thin Solid Films* **2009**, *517*, 5038–5043. [CrossRef]
141. Saji, V.S.; Choe, H.C.; Brantley, W.A. An electrochemical study on self-ordered nanoporous and nanotubular oxide on Ti–35Nb–5Ta–7Zr alloy for biomedical applications. *Acta Biomater.* **2009**, *5*, 2303–2310. [CrossRef]
142. Choe, H.-C.; Kim, W.-G.; Jeong, Y.-H. Surface characteristics of HA coated Ti–30Ta–xZr and Ti–30Nb–xZr alloys after nanotube formation. *Surf. Coat. Technol.* **2010**, *205*, S305–S311. [CrossRef]
143. Kim, E.-S.; Jeong, Y.-H.; Choe, H.-C.; Brantley, W.A. Formation of titanium dioxide nanotubes on Ti–30Nb–xTa alloys by anodizing. *Thin Solid Films* **2013**, *549*, 141–146. [CrossRef]
144. Wang, P.; Li, H.; Zhang, Y.; Liu, H.; Guo, Y.; Liu, Z.; Zhao, S.; Yin, J.; Guo, Y. Morphology of nanotube arrays grown on Ti–35Nb–2Ta–3Zr alloys with different deformations. *Appl. Surf. Sci.* **2014**, *290*, 308–312. [CrossRef]
145. Navarro-Laboulais, J.; Amigó-Mata, J.; Amigó-Borrás, V.; Igual-Muñoz, A. Electrochemical characterization and passivation behaviur of new beta-titanium alloys (Ti35Nb10Ta-xFe). *Electrochim. Acta* **2017**, *227*, 410–418. [CrossRef]
146. Bocchetta, P.; Sunseri, C.; Masi, R.; Piazza, S.; Di Quarto, F. Influence of initial treatments of aluminium on the morphological features of electrochemically formed alumina membranes. *Mater. Sci. Eng. C* **2003**, *23*, 1021–1026. [CrossRef]
147. Pawlik, A.; Rehman, M.A.U.; Nawaz, Q.; Bastan, E.F.; Sulka, D.G.; Boccaccini, A.R. Fabrication and characterization of electrophoretically deposited chitosan-hydroxyapatite composite coatings on anodic titanium dioxide layers. *Electrochim. Acta* **2019**, *307*, 465–473. [CrossRef]
148. Kunze, J.; Müller, L.; Macak, J.M.; Greil, P.; Schmuki, P.; Müller, F.A. Time-dependent growth of biomimetic apatite on anodic TiO_2 nanotubes. *Electrochim. Acta* **2008**, *53*, 6995–7003. [CrossRef]
149. Sarraf, M.; Razak, B.A.; Crum, R.; Gámez, C.; Ramirez, B.; Noor Hayaty Binti Abu, K.; Bahman, N.-T.; Vijay, G.; Nazatul Liana, S.; Wan, J.B. Adhesion measurement of highly-ordered TiO_2 nanotubes on Ti-6Al-4V alloy. In *Processing and Application of Ceramics*; National Library of Serbia: Belgrade, Serbia, 2017; Volume 11, pp. 311–321.
150. Fojt, J.; Hybasek, V.; Jarolimova, P.; Pruchova, E.; Joska, L.; Malek, J. Corrosion behaviour of the titanium beta alloy nanotubular surface in the presence of fluoride ions. *Koroze a Ochr. Mater.* **2019**, *63*, 72–78. [CrossRef]
151. Fojt, J.; Filip, V.; Joska, L. On the increasing of adhesive strength of nanotube layers on beta titanium alloys for medical applications. *Appl. Surf. Sci.* **2015**, *355*, 52–58. [CrossRef]
152. Carobolante, J.P.A.; Silva, K.B.; Munoz Chaves, J.A.; Dias, M.F.; Netipanyj, K.; Popat, C.; Alves Claro, S.P.R. Nanoporous layer formation on the Ti10Mo8Nb alloy surface using anodic oxidation. *Surf. Coat. Tech.* **2020**, *386*, 125467. [CrossRef]
153. Kim, W.-G.; Choe, H.-C. Nanostructure and corrosion behaviors of nanotube formed Ti-Zr alloy. *Trans. Nonferrous Metals Soc. China* **2009**, *19*, 1005–1008. [CrossRef]
154. Yu, W.-Q.; Qiu, J.; Xu, L.; Zhang, F.-Q. Corrosion behaviors of TiO_2 nanotube layers on titanium in Hank's solution. *Biomed. Mater.* **2009**, *4*, 012–065. [CrossRef] [PubMed]
155. Ossowska, A.; Sobieszcyk, S.; Supernak, M.; Zielinski, A. Morphology and properties of nanotubular oxide layer on the "Ti-13Zr-13Nb" alloy. *Surf. Coat. Technol.* **2014**, *58*, 1239–1248. [CrossRef]
156. Kaseem, M.; Choe, H. Electrochemical and bioactive characteristics of the porous surface formed on Ti-xNb alloys via plasma electrolytic oxidation. *Surf. Coat. Technol.* **2019**, *379*, 125027. [CrossRef]
157. Cordeiro, M.J.; Nagay, B.E.; Ribeiro, A.L.; da Cruz, N.; Rangel, E.; Fais, L.M.G.; Vaz, G.L.; Barao, R.A. Functionalization of an experimental Ti-Nb-Zr-Ta alloy with a biomimetic coating produced by plasma electrolytic oxidation. *J. Alloys Compd.* **2019**, *770*, 1038–1048. [CrossRef]
158. Say, W.C.; Chen, C.C.; Shiu, Y.H. Monitoring the effects of growing titania nanotubes on titanium substrate by electrochemical impedance spectroscopy measurement. *Jpn. J. Appl. Phys.* **2009**, *48*, 004–035. [CrossRef]
159. Guo, Y.; Chen, D.; Lu, W.; Jia, Y.; Wang, L.; Zhang, X. Corrosion resistance and in vitro response of a novel Ti35Nb2Ta3Zr alloy with a low Young's modulus. *Biomed. Mater.* **2013**, *8*, 055004. [CrossRef]
160. Marques, I.D.S.V.; Barão, V.A.R.; da Cruz, N.C.; Yuan, J.C.-C.; Mesquita, M.F.; Ricomini-Filho, A.P.; Sukotjo, C.; Mathew, M.T. Electrochemical behavior of bioactive coatings on cp-Ti surface for dental application. *Corros. Sci.* **2015**, *100*, 133–146. [CrossRef]
161. Beline, T.; da Silva Vieira Marques, I.; Matos, A.O.; Ogawa, E.S.; Ricomini-Filho, A.P.A.P.; Rangel, E.C.; da Cruz, N.C.; Sukotjo, C.; Mathew, M.T.; Landers, R.; et al. Production of a biofunctional titanium surface using plasma electrolytic oxidation and glow-discharge plasma for biomedical applications. *Biointerphases* **2016**, *11*, 11013. [CrossRef]
162. Wen, L.; Wang, Y.; Zhou, Y.; Guo, L.; Ouyang, H.J. Microstructure and corrosion resistance of modified 2024 Al alloy using surface mechanical attrition treatment combined with microarc oxidation process. *Corros. Sci.* **2011**, *53*, 473–480. [CrossRef]
163. Mazigi, O.; Kannan, B.M.; Xu, J.; Choe, C.H.; Ye, Q. Biocompatibility and degradation of a low elastic modulus Ti-35Nb-3Zr alloy: Nanosurface engineering for enhanced degradation resistance. *ACS Biomater. Sci. Eng.* **2017**, *3*, 509–517. [CrossRef] [PubMed]
164. Jáquez-Muñoz, J.M.; Tiburcio, C.G.; Miramontes, J.; Ángel, C.; López, F.E.; Robledo, P.Z.; Acuña, R.A.S.; Calderon, F.A. Electrochemical Behavior of Titanium Alloys Using Potentiodynamic Polarization. *ECS Trans.* **2021**, *101*, 173–178. [CrossRef]

165. Jáquez-Muñoz, J.M.; Gaona-Tiburcio, C.; Cabral-Miramontes, J.; Nieves-Mendoza, D.; Maldonado-Bandala, E.; Olguín-Coca, J.; López-León, L.D. Flores-De los Rios, J.P.; Almeraya-Calderón, F. Electrochemical Noise Analysis of the Corrosion of Titanium Alloys in NaCl and H_2SO_4 Solutions. *Metals* **2021**, *11*, 105. [CrossRef]
166. Zhou, H.; Li, F.; He, B.; Wang, J.; Sun, B. Air Plasma Sprayed Thermal Barrier Coatings on Titanium Alloy Substrates. *Surf. Coat. Technol.* **2007**, *201*, 7360–7367. [CrossRef]
167. Zherebtsov, S.; Salishchev, G.; Łojkowski, W. Strengthening of a Ti-6Al-4V Titanium Alloy by Means of Hydrostatic Extrusion and other Methods. *Mater. Sci. Eng. A* **2009**, *515*, 43–48. [CrossRef]
168. Liu, Y.Z.; Zu, X.T.; Wang, L.; Qiu, S.Y. Role of Aluminum Ion Implantation on Microstructure, Microhardness and Corrosion Properties of Titanium Alloy. *Vacuum* **2008**, *83*, 444–447. [CrossRef]
169. Wang, Y.M.; Guo, L.X.; Ouyang, J.H.; Zhou, Y.; Jia, D.C. Interface Adhesion Properties of Functional Coatings on Titanium Alloy Formed by Microarc Oxidation Method. *Appl. Surf. Sci.* **2009**, *255*, 6875–6880. [CrossRef]
170. Vadiraj, A.; Kamaraj, M. Effect of Surface Treatments on Fretting Fatigue Damage of Biomedical Titanium Alloys. *Tribol. Int.* **2007**, *40*, 82–88. [CrossRef]
171. He, Z.Y.; Wang, Z.X.; Wang, W.B.; Fan, A.L.; Xu, Z. Surface Modification of Titanium Alloy Ti6Al4V by Plasma Niobium Alloying Process. *Surf. Coat. Technol.* **2007**, *201*, 5705–5709. [CrossRef]
172. Cassar, G.; Avelar-Batista Wilson, J.C.; Banfield, S.; Housden, J.; Matthews, A.; Leyland, A. A Study of the Reciprocating-Sliding Wear Performance of Plasma Surface Treated Titanium Alloy. *Wear* **2010**, *269*, 60–70. [CrossRef]
173. Singh, A.V.; Rosenkranz, D.; Ansari, M.H.D.; Singh, R.; Kanase, A.; Singh, S.P.; Johnston, B.; Tentschert, J.; Laux, P.; Luch, A. Artificial Intelligence and Machine Learning Empower Advanced Biomedical Material Design to Toxicity Prediction. *Adv. Intell. Syst.* **2020**, *2*, 2000084. [CrossRef]
174. Ye, D.; Wang, W.; Xu, Z.; Yin, C.; Zhou, H.; Li, Y. Prediction of Thermal Barrier Coatings Microstructural Features Based on Support Vector Machine Optimized by Cuckoo Search Algorithm. *Coatings* **2020**, *10*, 704. [CrossRef]
175. Singh, A.V.; Jahnke, T.; Wang, S.; Xiao, Y.; Alapan, Y.; Kharratian, S.; Onbasli, M.C.; Kozielski, K.; David, H.; Richter, G.; et al. Anisotropic Gold Nanostructures: Optimization via in Silico Modeling for Hyperthermia. *ACS Appl. Nano Mater.* **2018**, *1*, 6205–6216. [CrossRef]
176. Karballaeezadeh, N.; Mohammadzadeh, S.D.; Moazemi, D.; Band, S.S.; Mosavi, A.; Reuter, U. Smart Structural Health Monitoring of Flexible Pavements Using Machine Learning Methods. *Coatings* **2020**, *10*, 1100. [CrossRef]
177. Richard, C.; Kowandy, C.; Landoulsi, J.; Geetha, M.; Ramasawmy, H. Corrosion and Wear Behavior of Thermally Sprayed Nano Ceramic Coatings on Commercially Pure Titanium and Ti–13Nb–13Zr Substrates. *Int. J. Refract. Met. Hard Mater.* **2010**, *28*, 115–123. [CrossRef]